NEDO-25[illegible]-1
80NA [illegible]4
Class
November 1980

TN-317

MARK II CONTAINMENT PROGRAM

COMPARISON OF SINGLE AND MULTIVENT CHUGGING - PHASE 2

J. A. Block - Creare Inc.
F. X. Dolan - Creare Inc.
B. R. Patel - Creare Inc.

Approved: _____
B. R. Patel, Project Director
Creare Incorporated

Approved: _____
J. A. Block, President
Multiphase Division
Creare Incorporated

Approved: _____ FOR
P. W. Ianni, Manager
Containment Design

Approved: _____
H. E. Townsend, Manager
Containment Technology

This document was prepared for the Mark II Utility Owners Group by Creare Incorporated under contract with of the General Electric Company.

NUCLEAR POWER SYSTEMS DIVISION • GENERAL ELECTRIC COMPANY
SAN JOSE, CALIFORNIA 95125

GENERAL ELECTRIC

DISCLAIMER OF RESPONSIBILITY

The only undertakings of the General Electric Company respecting information in this document are contained in the contracts for Mark II Containment Consulting Services between the General Electric Company and each of the members of the U.S. Mark II Owners Group, effective variously June 9,1975, June 13,1975, or July 29,1975, and nothing contained in this document shall be construed as changing the contracts. The use of this information by anyone other than the members of the U.S. Mark II Owners Group either themselves or through their technical consultants, or for any purpose other than that for which it is intended under the contracts, is not authorized; and with respect to any unauthorized use, the General Electric Company makes no represenation or warranty, express or implied, and assumes no liability of any kind as to the completeness, accuracy, usefulness or non-infringing nature of the information contained in this document.

CONTENTS

TABLES

ILLUSTRATIONS

EXECUTIVE SUMMARY

This interim report presents data obtained in Phase 2 of the Scaled Multivent Test Program.

The objectives of the Scaled Multivent Test Program are to, (1) demonstrate that single cell loads are bounding by establishing that multivent loads are less than single vent loads, (2) determine the trend in loads with number of vents and demonstrate validity by experiments at several scales, and (3) obtain data which may be used to confirm analytical application methods. The program contains single vent tests at four scales (with CONMAP and 4T providing fifth and sixth scales) and multivent tests at two scales as summarized in Table S-1. Data from the 1/4 and 5/12 scale single vent tests and a portion of the 1/10 and 1/6 multivent tests are presented in this report.

The five test vessels used ranged in size from 10 to 44 inches in diameter. All geometries had the drywell-over-wetwell configuration of Mark II plants with straight vents. Critical dimensions such as submergence, vent-to-pool floor clearance, vent diameter, vent spacing and wetwell diameter were linearly scaled; and the vent lengths and the pool-to-vent area ratio were kept constant between geometries.

Special tests in this program, together with previous programs provide data on the effects of varying these dimensions. In this program chugging data were obtained over a wide range of conditions (steam flux, air content, pressure, pool temperature) to contribute to basic understanding of the physics of the phenomena and hence the effect of scale and the extension of the data to full scale.

Extensive instrumentation, together with a 28 channel analog tape recorder and a 64 channel minicomputer-based data acquisition and reduction system provided data on pool interior and boundary pressures, pool temperature distribution, vent pressures; water position and velocity in the vents, vent, vessel and basemat accelerations, and the various steady-state test conditions such as

steam and air flow rates, system pressure and pool temperature and depth. Data reduction was accomplished by manually-guided computer manipulations.

The principle test results obtained from Phase 2 are:

a. Mean pool boundary pressures in multivent geometries are less than the mean pool boundary pressure in the single vent geometry of the same scale.

b. Trends in mean peak overpressure (POP), mean peak underpressure (PUP), and mean chug frequency with variation in test conditions observed in the single and multiple vent tests of Phase 2 are similar to the trends observed in the Phase 1 tests.

Phase 2 has further contributed toward meeting the objectives of this program.

Table S-1

SCALED MULTIVENT TEST PROGRAM

Single Vent Test Geometries	1/10*, 1/6*, 1/4**, 5/12** scales
Multivent Test Geometries	1/10 scale 3*, 7*, 19** vents 1/6 scale 3*, 7** vents
Additional Test Geometries	Effect of drywell volume* Effect of pool size* Effect of vent location in the pool* Effect of vent length**

Total Number of Test Geometries = 19
Total Number of Tests = 749

*Tests performed in Phase 1.
**Tests performed in Phase 2.

1. INTRODUCTION

This is an interim data report on the Scaled Multivent Test Program. This program has provided a significant data base on chugging in single and multiple vent geometries at several scales. The data base was generated in two phases. Phase 1 results were presented in Reference 1. This data report discusses the results of the Phase 2 program and draws on results from the Phase 1 program to make logical connections between the two data bases.

1.1 BACKGROUND

After the initial pool swell transient during a postulated LOCA in a pressure suppression containment system, steam with decreasing amounts of air is vented from the drywell into the wetwell pool via the vent system. This condenses the steam in the wetwell pool and limits the pressure buildup in the containment. During such steam venting, condensation-driven oscillations have been observed in various experiments (see Reference 2).

Two types of condensation-driven oscillations have been observed (see Reference 2). The first type, called "condensation oscillations", occur during the earlier portion of the blowdown and are characterized by fairly sinusoidal pressure oscillations in the entire drywell, vent and wetwell system. These condensation oscillations are followed by the second type of condensation-driven oscillations called "chugging". Chugging is characterized by discrete bursts of pressure oscillations in the wetwell pool with quiescent periods between them. The pressure oscillations during chugging are associated with the rapid collapse of the steam "bubble" at the vent exit and typically exhibit a pressure spike followed by a damped ringout which has predominant frequency components at the vent and pool natural frequencies.

An overview of the Mark II chugging program is shown in Figure 1-1. The Mark II Lead Plant Chugging Loads Justification Report (see Reference 3) provided a technical basis for permitting the licensing review of the lead Mark II plants to proceed in advance of confirmatory analytical and testing efforts. That report demonstrated that design loads were conservatively bounded by the

full-scale single-cell loads measured in the 4T facility tests (see Reference 2). The Scaled Multivent Test Program was initiated to provide experimental confirmation of the bounding nature of single-cell loads.

Containment loads for assessment of later Mark II plants may be calculated from the improved chugging load definition methodology currently under development in Mark II Task A.16 or by alternate methods. The methods use full-scale single-cell 4T data and extend their application to multivent Mark II plants.

1.2 SCALED MULTIVENT TEST PROGRAM OVERVIEW

The detailed program plan and description of the Scaled Multivent Test Program are given in References 4 and 5 and will be briefly summarized here.

The main objectives of the Scaled Multivent Test Program were to determine multivent effects on chugging (such as trends in pool wall pressure magnitudes with number of vents), to demonstrate that multivent loads are less than single vent loads, and to provide a data base for assessment of analytical load application techniques.

To meet these objectives tests in single vent geometries at four scales (1/10, 1/6, 1/4, and 5/12 scale) and multivent geometries at two scales (3, 7, and 19 vents at 1/10 scale and 3 and 7 vents at 1/6 scale) were included in the Scaled Multivent Test Program. Special tests to determine the effects of drywell volume, pool size, and vent location in the pool were also included. The testing was divided into two phases as shown in Figure 1-2. The overall program schedule is shown in Table 1-1.

Phase 1 included the design and construction of the test facility (Subsection 2.1), the instrumentation (Subsection 2.3), and the data acquisition (Subsection 3.1) and reduction hardware and software (Subsection 3.2). After a shakedown of the complete facility including instrumentation, data acquisition and reduction systems tests were performed on the 14 Phase 1 geometries. Five of these 14 geometries provided the Phase 1 portion of the baseline single and multivent test data. These five geometries were the 1, 3 and 7 vent configurations at

1/10 scale and 1 and 3 vent configurations at 1/6 scale. The remaining geometries tested in Phase 1 provided data on the effects of drywell volume, pool size and vent location in the pool.

In Phase 2 an additional test vessel was installed in the test facility, and five single and multiple vent geometries were tested. These were two more single vent geometries at 1/4 and 5/12 scale, a single vent geometry at 5/12 scale having increased vent length and two additional multivent geometries (19 vents at 1/10 scale and 7 vents at 1/6 scale). The test matrices (Section 4) for Phase 1 and Phase 2 covered a wide range of test parameters such as steam mass flux, pool temperature, steam air content, and wetwell airspace pressure.

The test data and results of the Phase 2 program are presented in Sections 5 and 6, along with some results from the related Phase 1 baseline geometries. A final report will be issued in the third quarter of 1980 that will include results of the detailed data analyses currently being performed.

Table 1-1

SCHEDULE - SCALED MULTIVENT TEST PROGRAM

Activity	1978				1979				1980			
	1	2	3	4	1	2	3	4	1	2	3	4
Phase 1												
• Facility Construction & Shakedown	▬	▬	▬	▬								
• Phase 1 Tests & Analyses				▬	▬	▬						
• Phase 1 Test Report									▼			
Phase 2												
• Phase 2 Tests						▬	▬	▬				
• Analyses								▬	▬	▬		
• Final Report											▼	

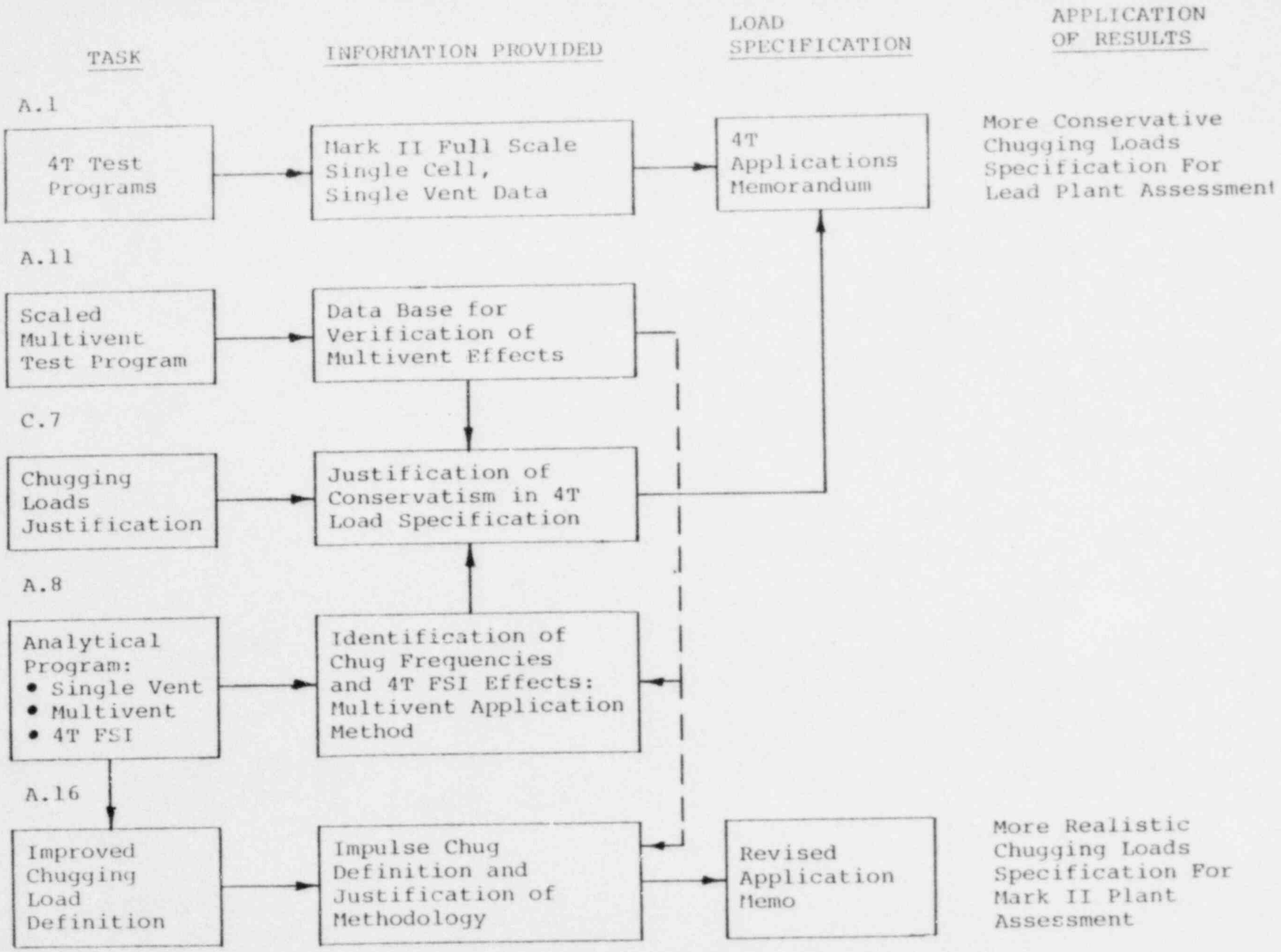

Figure 1-1. Mark II Chugging Programs Overview

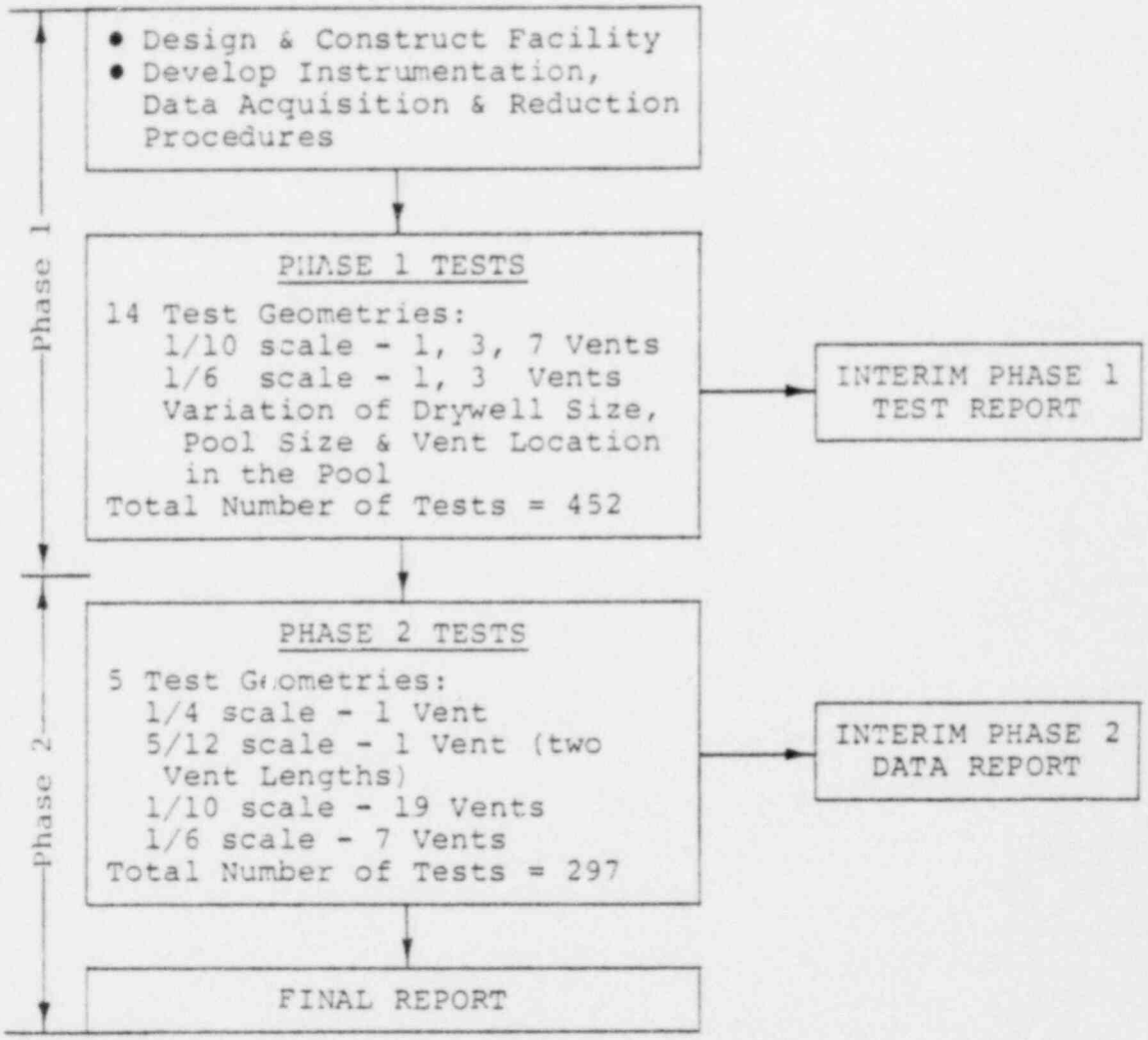

Figure 1-2. Scaled Multivent Test Program Overview

2. TEST FACILITY AND INSTRUMENTATION

In this section the test facility, test geometries and instrumentation used in Phase 2 are described.

2.1 TEST FACILITY AND GEOMETRIES

The Scaled Multivent Test Facility is shown schematically in Figure 2-1. It includes steam, water and air supply systems and five test vessels used for the single and multiple vent geometries. Of the five vessels, two were used for Phase 2.

Steam was provided from a 20,000 lb/hr, 200 psi boiler with a full flow discharge pressure regulator and flow control valves. The steam flow rate into the drywells was measured with standard orifice meters, with three meters provided for each test geometry to cover the wide range of flows required in the test matrix. One of the meters (in a 4-in Schedule 40 pipe) was located downstream from the boiler pressure regulator and delivered steam to a 6-in header from which the steam was distributed to the geometry under test. Two "portable" steam flow meters (in a 2-in Schedule 40 pipe) were located close to the vessel under test to minimize condensation losses from the point of flow measurement to the drywell, at low flow rates. Steam condensation between the flow meters and the drywells was estimated to be less than 5% of the metered steam flow rate for the geometry under test. A constant steam flow was maintained independent of drywell pressure fluctuations by using a choked valve at the steam inlet to the drywell. Coolant water was supplied to the vessel under test to maintain the desired pool temperature and vent submergence. The coolant water was pumped from large storage tanks to a header system which connected to each of the test vessels through isolation valves. The return coolant was pumped from the vessel through connections located approximately 3-in below the pool surface and was circulated back to the supply tanks through a cooling tower.

Air for pressurizing the test vessels and for mixing with the vent steam flow was provided by an air compressor. The system was capable of supplying up to 0.4 lb/sec of air at 90 psig. The flow rate of air to the drywell was measured with turbine meters, and a constant flow rate was maintained by a choked flow control valve at the inlet to the drywell.

The scaled geometries tested in Phase 2 are shown in Table 2-1 along with the as-built critical dimensions. The dimensions of the reference Mark II containment from which tests test geometries were scaled* are shown in Table 2-2. The scale factor is defined as the ratio of the scaled vent diameter to the nominal vent diameter (24-in). The vent submergence and clearance were scaled linearly. Drywell volume was scaled by the cube of the scale factor and the pool to vent area ratio was preserved at the prototypical value.

The five geometries tested in Phase 2 are shown schematically in Figures 2-2 through 2-5. The wetwell vessel for the 5/12 scale single vent and 1/6 and 1/10 multivent geometries was a custom-fabricated, 44-in i.d. and 3/4-in wall thickness pressure vessel. For the 1/4 scale single vent geometry, a 28-in Schedule 40 (27.25-in i.d. and 3/8-in wall thickness) steel pipe was used to fabricate the wetwell vessel. Drywells for these geometries were mounted on top of the wetwell vessel with straight vents, similar to the Mark II configuration. For the 5/12 scale vent tests, coolant water was supplied through 12 2-in diameter connections spaced uniformly around the circumference of the vessel, near the bottom. In all of the other test vessels, the coolant was supplied through a single connection on the bottom of the vessel and flowed into the pool through narrow slits around the periphery of the bottom plate. These slight differences in water supply technique are not expected to have any measureable effect on pool temperature distribution.

In the 1/10 and 1/6 scale multivent geometries the vent diameters were 2.32-in (2.5-in Schedule 80 pipe) and 3.83-in (4-in Schedule 80 pipe), the same as in the Phase 1 program. In the 1/4 scale geometry the vent diameter was 6.06-in

*The scaling rationale is discussed in Reference 4.

(6-in Schedule 40 pipe) and in the 5/12 scale geometry it was 10.02-in (10-in Schedule 40 pipe). The pool-to-vent area ratio was maintained at 19.5±5% for all Phase 2 geometries as in the Phase 1 program.

The layout of the multiple vents in the wetwell pools was designed to produce the following features:

a. Constant vent-to-vent spacing for all configurations at a single scale.

b. Nearly constant vent-to-wall pressure measurement spacing.

c. Hexagonal cells that were constant in size for a given scale and whose total area relates in a reasonably constant fashion to pool area.

Figures 2-6 and 2-7 show the single and multiple vent layouts at 1/10 and 1/6 scale for both Phase 1 and Phase 2 geometries. The multivent layouts were constructed by maintaining the size of a hexagonal cell surrounding the vents equal to the hexagonal cell which fits inside the single vent wetwell. The use of the hexagonal cell concept aids in visualizing the arrangement of vents in the pool and provides for a similarity in vent layout among the several multivent geometries. The ratio of the total hexagonal cell area to the pool area was approximately the same from configuration to configuration. The pool-to-vent area ratio for the 19 vents at 1/10 scale was 18.9, and the hexagonal cell to pool area fraction was 0.815. In the 7 vents at 1/6 scale, these geometry parameters were 18.9 and 0.89, respectively.

Vent lengths were chosen to be approximately 9-ft for all configurations except Geometry R (see Table 2-1 for geometry descriptions) in which the effect of increased vent length (17-ft) was investigated. This length provided the best match to the requirement for multiple use of several of the test vessels. In the multivent geometries of Phase 2, the vent length was the same as the single and multivent geometries at the same scale tested in Phase 1. All vents

extended above the diaphragm plate separating the drywell from the wetwell by at least six inches. The vents were welded to the diaphragm plate and were supported in the wetwell with struts which centered the vent assembly within the pool and provided lateral stiffness. In the case of multiple vent geometries, each vent was also tied to the adjacent vents with struts. These struts were 1/2-in thick by 3-in wide steel plate (4-in wide in the case of the 5/12 scale vent) welded to the vent pipes, and located near or above the top of the normal pool level for each scale.

2.2 TEST PROCEDURES

Tests in Phase 2 were run in a steady-state mode in which coolant water was supplied to the wetwell pool to maintain a constant mean pool temperature at a fixed steam mass flux, steam air-content and wetwell airspace pressure. The pool level, and hence vent submergence, was controlled manually by adjusting the coolant return rate. Steam and air were supplied to the drywell through choked flow control valves.

A test was initiated by establishing steady values of the wetwell airspace pressure, steam mass flux, steam air-content, pool temperature and pool level. All of these parameters were monitored by the computer-based data acquisition system and reduced and displayed in real-time to assist the operators in adjusting the test conditions within predetermined tolerances. Following several minutes of steady operation, the main data acquisition sequence was initiated and data were collected for around 100 seconds. At the end of the test, average values of the critical test parameters during the test were printed out from the computer and checked against the desired test conditions.

Under certain conditions it was not possible to maintain a steady pool temperature and the test was run in a transient pool temperature mode. Generally, this occurred at low steam mass fluxes and low subcoolings (high pool temperature) where significant thermal stratification occurred within the pool, and an occasional sharp chug would cause rapid mixing in the pool. For these tests, the coolant flow rate through the pool was set slightly lower than that needed

to maintain thermodynamic equilibrium and the data acquisition sequence was initiated when the indicated pool temperature was approximately 10°F below the desired nominal value. During the course of the 100 second data acquisition sequence, the temperature would usually rise to about 10°F above the nominal value.

Under some test conditions no chugging occurred, i.e. no appreciable pressure oscillations were observed. This was at a low steam mass flux and high subcooling (cold pool) where steady condensation occurred at the steam/water interface near the vent exit. During these tests no data were recorded.

2.3 INSTRUMENTATION

The Scaled Multivent Test Facility was provided with sufficient instruments to obtain the measurements required to meet the objectives of the test program. These measurements were classified into two main categories, principal and system. The principal data consisted of pool wall pressures, "source" pressures, pool temperatures, wall and vent accelerations, vent static pressure and vent water level. In addition to pool pressures and temperature distributions, these data were used to assist in a better understanding of chugging and multivent effects. The system data were needed to establish the test conditions such as steam and air flow rates to the drywell, drywell pressures and temperatures, vent submergence, and wetwell freespace pressure and temperature. A schematic diagram of the measurement locations is given in Figure 2-8 and the instrument specifications, cross-referenced to Figure 2-8, are given in Table 2-3.

2.3.1 Principal Data

Pool Wall Pressures - Pool wall pressures were measured using flush-mounted, fast response pressure transducers which were protected from thermal transients without loss of frequency response. The pool wall pressures were measured at these four horizontal planes in the pool.

a. Approximately 1-in above pool bottom elevation.

b. Mid-clearance elevation.

c. One vent diameter below vent exit elevation at three circumferential positions.

d. Mid-submergence elevation.

Pool Temperatures - The pool temperature measurements were made with grounded junction copper-constantan thermocouples having a time constant of less than one second in water. Temperatures in the pool were measured at 12 locations for the single vent geometries and the 19 vent 1/10 scale geometry and at 13 locations for the 1/6 scale seven vent geometry. The temperature measurement locations were:

a. One thermocouple 3-in above the pool bottom.

b. One thermocouple at the mid-clearance elevation.

c. Up to five thermocouples located at one vent diameter below the vent exit. Three thermocouples were mounted on a rake to provide a radial temperature profile. In the single event and 1/10 scale geometries only two radial thermocouple were used at this elevation; the innermost thermocouple was eliminated to avoid possible interference with the steam bubble dynamics at the vent exit. Also, at this same elevation, two more thermocouples were located equally spaced around the circumference of the vessel.

d. Five thermocouples were located at the vent mid-submergence elevation, three on a radial rake and two more at equally spaced circumferential positions.

e. One thermocouple 3-in below the pool surface elevation.

Vent, Pool Wall and Basemat Accelerations - The accelerations were measured using piezoelectric accelerometers at these three locations:

a. Accelerometer (up to 3) located on the vent(s), one vent diameter above the vent exit, the sensitive axis on a plane perpendicular to the vent pipe axis.

b. One accelerometer located on the wall of the vessel at one vent diameter below the vent exit, with the sensitive axis horizontal.

c. One accelerometer located on the vessel support ring which is used to secure the test vessel to the concrete basemat.

Chugging "Source" Pressures - Pressures (up to 3) in the pool were measured using fast response pressure transducers having specifications similar to those used for the wall pressure measurements. These transducers were supported with 3/4-in diameter wands projecting radially into the pool through the walls of the vessels at a point one vent diameter below the exit of the vents. The radial position of these probes was mid-way between the wall and the outside diameter of the vent pipe.

Vent Static Pressures - Vent static pressures were measured in up to three vents with fast response transducers which were mounted flush with the inside surface of the vents and approximately 8 vent diameters above the vent exits. These transducers were protected against thermal transients.

Vent Water Levels - Vent water levels were measured in up to three vents using a coupled conductivity probe system. Twenty-four probes were provided per vent, spaced 3-in apart along the length of the vent, starting 1-in above the vent exit.

Drywell Pressure - The fluctuating component of the drywell pressure (caused by the rapid condensation during a chug) was measured with a fast response piezoelectric pressure transducer installed in the drywell wall.

2.3.2 System Data

Wetwell Airspace Measurements - The wetwell airspace pressure was measured with a differential pressure transducer referenced to ambient. A mercury barometer was used to measure the atmospheric pressure and convert gauge pressure to absolute values. The temperature in the airspace was measured with a thermocouple extending approximately 4-in into the airspace and several feet above the nominal pool surface.

Steam Mass Flow Rate - The steam mass flow rate into the drywell was kept constant by using a choked flow control valve at the drywell vessel. Standard orifice meters were designed in accordance with ASME practice (see Reference 6). The steam pressure at the inlet to the meter was measured with a pressure transducer referenced to ambient, and the temperature was measured with a thermocouple installed in the steam line. The pressure drop across the orifice was measured with a differential pressure transducer, using condensate pots to ensure constant static levels on each leg of the transducer.

Pool Temperature - The pool temperature was one of the controlled system parameters and the measurement used to define pool temperature was taken from the thermocouple which was located at vent mid-submergence elevation and several inches from the pool wall (see Paragraph 2.3.1).

Air Mass Flow Rate - Air mass flow rate to the drywell was measured with turbine meters. Three turbine meters were available to cover the range of flow rates required in the test matrix. The pressure and temperature of the air supply to the turbine meters were measured with a pressure transducer and thermocouple, respectively.

Drywell Measurements - In addition to the fluctuating pressure component measured as principal data, the average drywell pressure and temperature were also measured using a pressure transducer and thermocouple.

Vent Submergence - The vent submergence (water depth above the vent exit) was controlled during the tests. Pool level was measured using a differential pressure transducer connected between the wetwell airspace and the pool. The vent submergence was determined from the total pool depth data and measured vent clearance.

In addition to the instruments discussed above, the test operator had various panel meter readouts and pressure gauges available to assist in setting and controlling test conditions. Although data from these indicators were not used in any data reduction procedures, they did provide a check on the operation of the data acquisition system.

2.3.3 Instrument Calibration and Measurement Accuracy

All of the pressure transducers and thermocouples used for principal and system data collection were calibrated in accordance with the schedule and procedures outlined in Reference 5. Table 2-3 shows the calibration accuracy for the major instruments used for principal and system data collection. The column headed "Total Measurement Accuracy" includes the effects of individual instrument calibration accuracy, data acquisition system accuracy and short-term gain stability. The last column in Table 2-3 shows the allowable tolerance band on the average value of the measured or derived parameter over the test duration. If the average of the parameter measured during a test fell outside the tolerance band, the test was repeated.

Table 2-1

SCALED MULTIVENT TEST PROGRAM - PHASE 2 TEST GEOMETRIES

Geometry Code*	Geometry Numbers**	Vent Dia (in)	Scale	Number of Vents	Vent Length (ft)	Wetwell Dia (in)	Drywell Volume (ft^3)	Vent Clearance (in)	Vent Submergence (in)	Pool to Vent Area Ratio
R	15	10.02	5/12	1	17	44	190	60	60	19.3
S	16	10.02	5/12	1	9.7	44	195	60	60	19.3
T	17	6.06	1/4	1	9.0	27.25	41.5	36	36	20.2
U	18	2.32	1/10	19	9.5	44	46.5	14	14	18.9
V	19	3.83	1/6	7	8.7	44	77	23	23	18.9

*See Table 4-2 for use of Geometry Code.

**Geometries 1 through 14 were tested in Phase 1 (See Reference 1)

Table 2-2

PROTOTYPICAL MARK II CONTAINMENT GEOMETRY PARAMETERS

Parameter	Reference Dimension
Vent Diameter	24 in
Vent Length	42 ft
Drywell Volume	2655 ft^3/vent
Vent Clearance	12 ft
Vent Submergence	12 ft
Pool to Vent Area Ratio	19.5

Table 2-3

INSTRUMENT LIST

Measured Parameter	Identification*	Instrument Type	Instrument Calibration Accuracy	Total Measurement Accuracy	Rise Time	Tolerances On Set Conditions
Steam Supply Pressure	P1	Pressure Gauge and Transducer	±0.5 psi	±1.0 psi	-	-
Orifice Meter Differential Pressure	P2	Differential Pressure Transducer	±0.5" H_2O	±0.6" H_2O	-	-
Steam Supply Temperature	T1	Thermocouple	±2°F	±4°F	-	-
Steam Flow	F1	Orifice Meter	±2%	±6%	-	±10%
Air Supply Pressure	P3	Pressure Gauge and Transducer	0.5 psi	±1.0 psi	-	-
Air Supply Temperature	T2	Thermocouple	±2°F	±4°F	-	-
Airflow	F2	Turbine Meters	±5%	±10%	-	±10%
Drywell Average Pressure	P4	Pressure Gauge and Transducer	±0.5 psi	±3 psi	-	-
Drywell Instantaneous Pressure	P5	Pressure Transducer	±0.5 psi	±1 psi	<2 msec	-
Wetwell Airspace Pressure	P6	Pressure Gauge and Transducer	±0.5 psi	±1 psi	-	±2 psi
Pool Wall Pressure	P7-12	Pressure Transducer	±0.5 psi	±1 psi	<50μ sec	-
"Source" Pressure	P13-15	Pressure Transducer	±0.5 psi	±1 psi	<50μ sec	-
Vent Static Pressures	P16-18	Pressure Transducer	±0.5 psi	±1 psi	<50μ sec	-

Table 2-3

INSTRUMENT LIST (Continued)

Measured Parameter	Identification*	Instrument Type	Instrument Calibration Accuracy	Total Measurement Accuracy	Rise Time	Tolerances On Set Conditions
Drywell Temperature	T3	Thermocouple	±4°F	±8°F	<10 sec	-
Wetwell Airspace Temperature	T4	Thermocouple	±4°F	±10°F	<10 sec	-
Pool Temperatures	T5-16	Thermocouple	±4°F	±8°F	<1 sec	±15°F
Vent Water Level	C1-3	Coupled Cond. Probes (24 per vent)	-	±4"	<2 msec	-
Wetwell Water Level	L1	Differential Pressure Transducer	±1.5" H_2O	±3"	-	±3" Average
Pool Wall Acceleration	A1	Accelerometer	±5%	±10%	**	-
Basemat Acceleration	A2	Accelerometer	±5%	±10%	**	-
Vent Accelerometer	A3-5	Accelerometer	±5%	±10%	**	-

*See Figure 2-8

**Frequency response of 5 kHz.

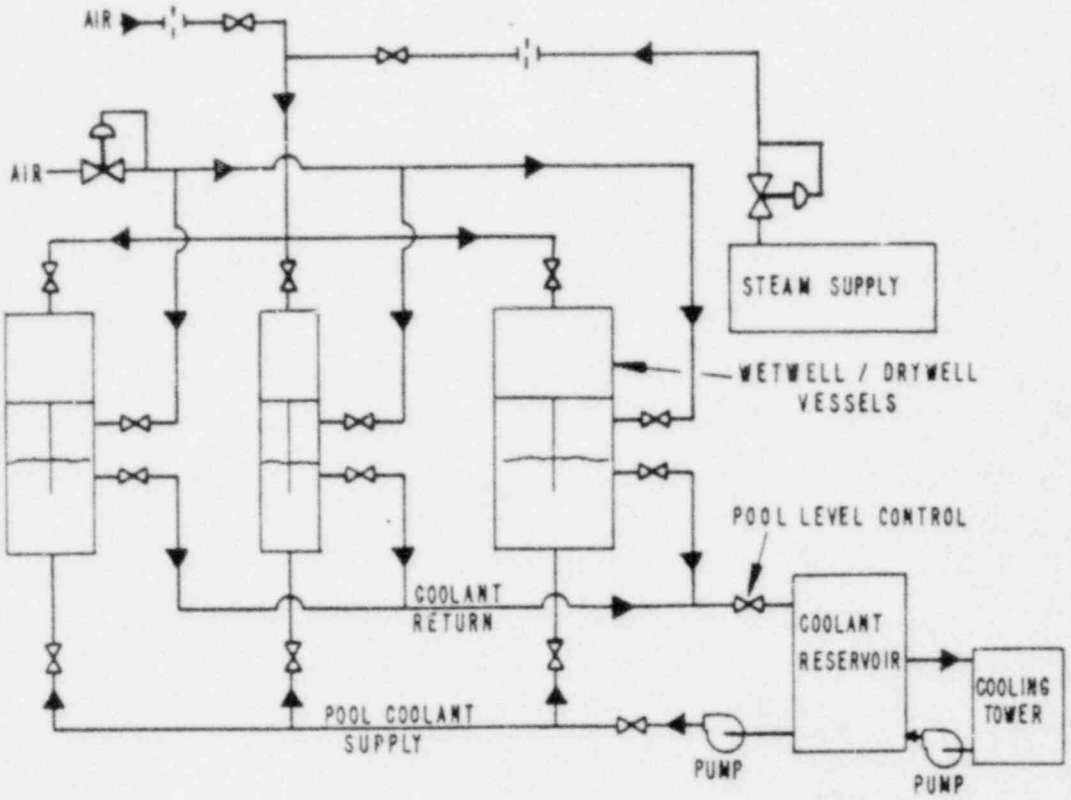

Figure 2-1. Schematic of the Scaled Multivent Test Facility

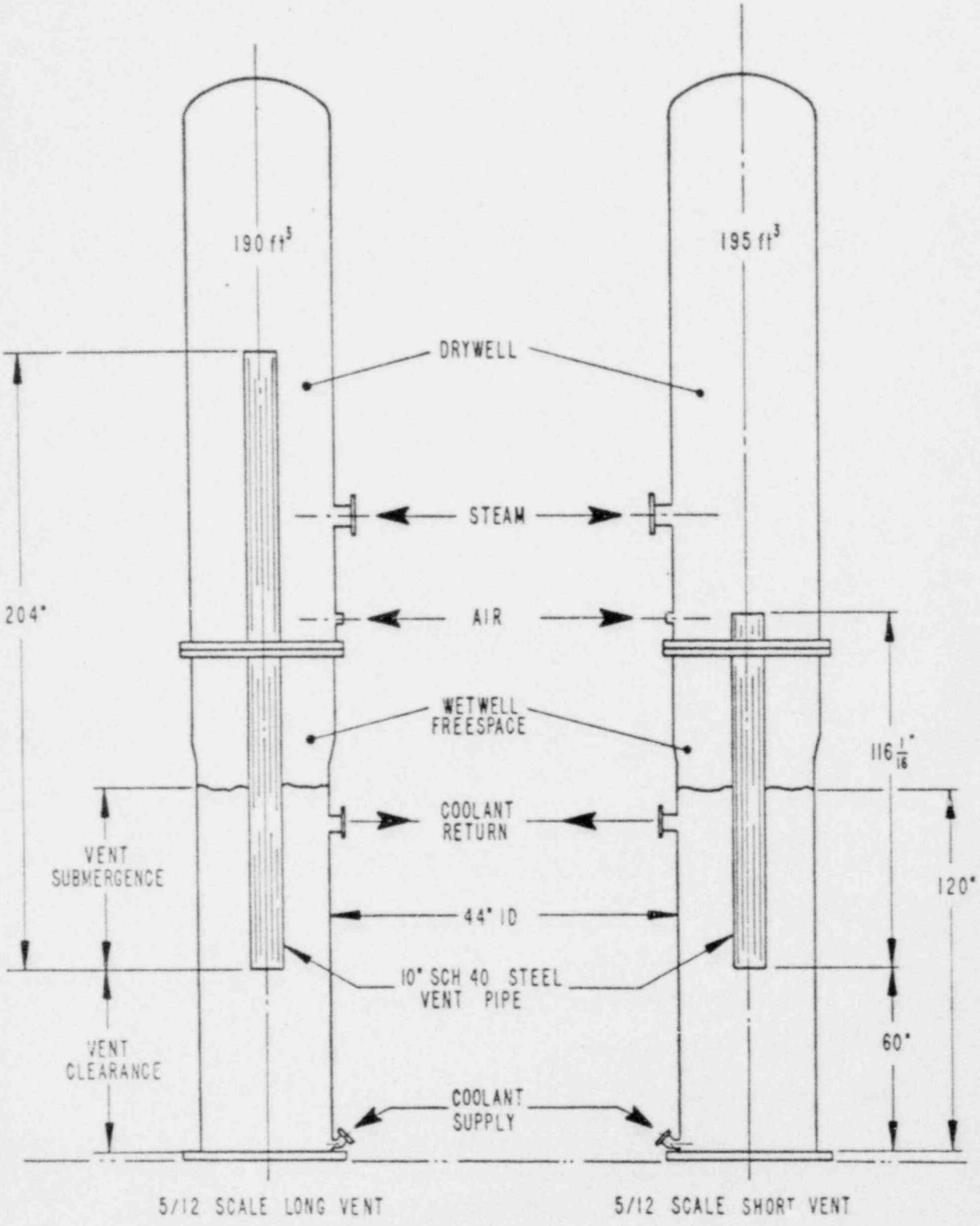

Figure 2-2. Scaled Multivent Test Program - Phase 2 5/12 Scale Single Vent Geometries

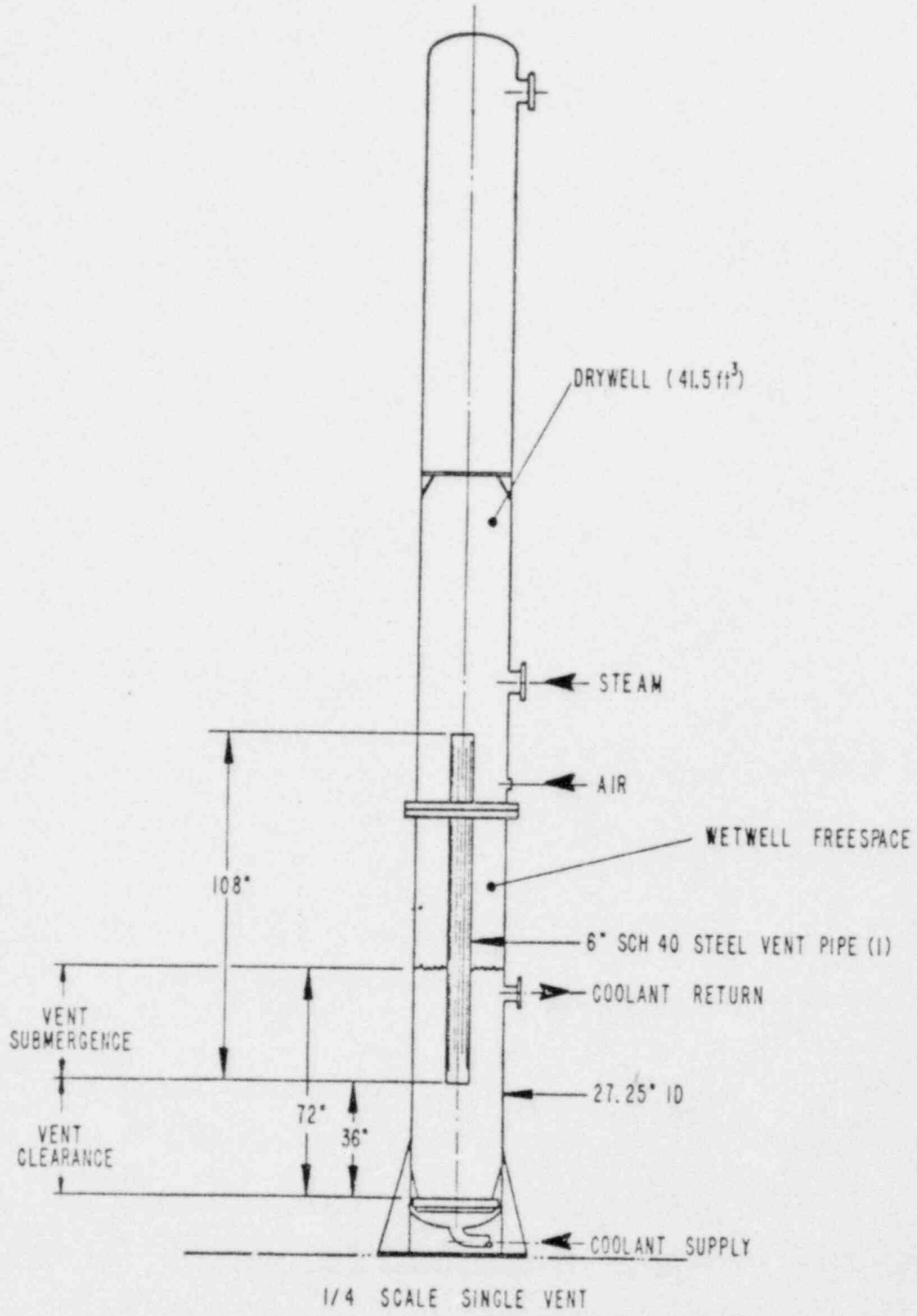

Figure 2-3. Scaled Multivent Test Program - Phase 2 1/4 Scale Single Vent Geometry

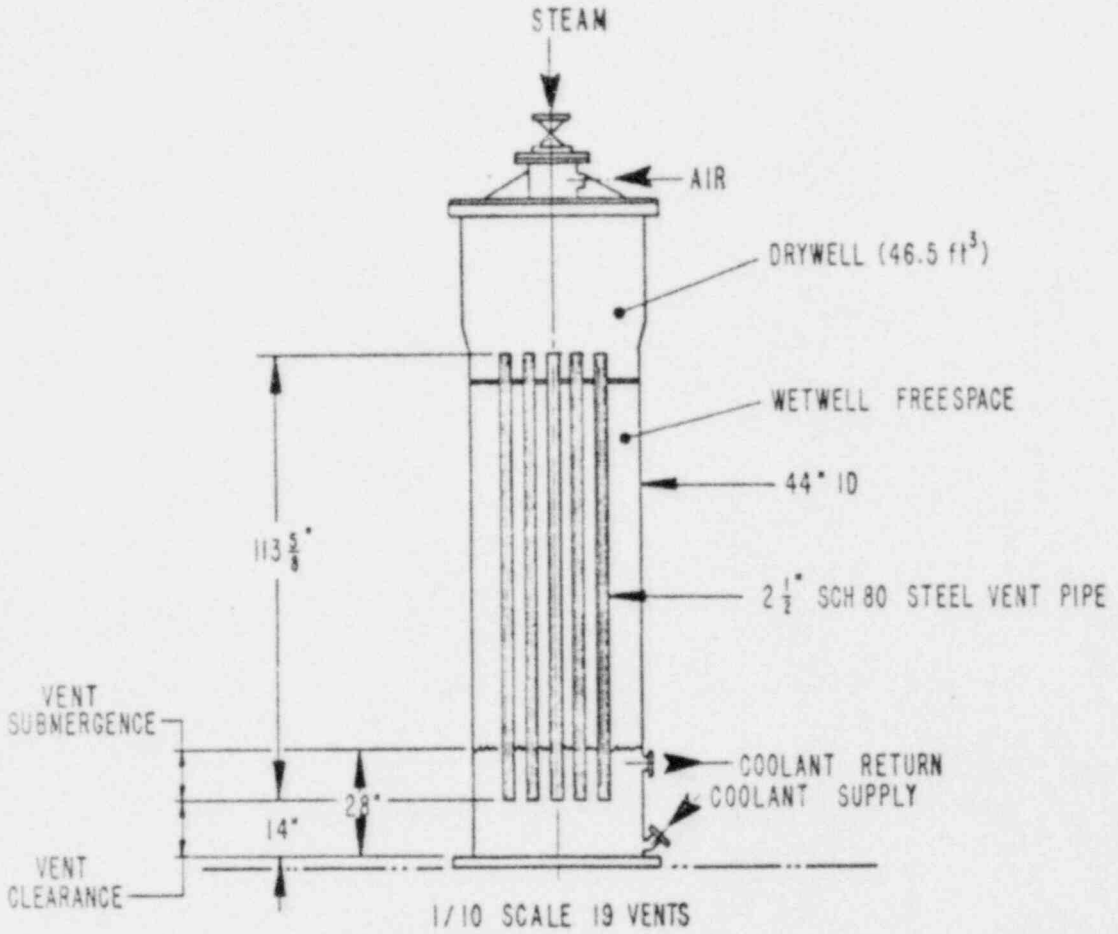

Figure 2-4. Scaled Multivent Test Program - Phase 2 1/10 Scale 19 Vent Geometry

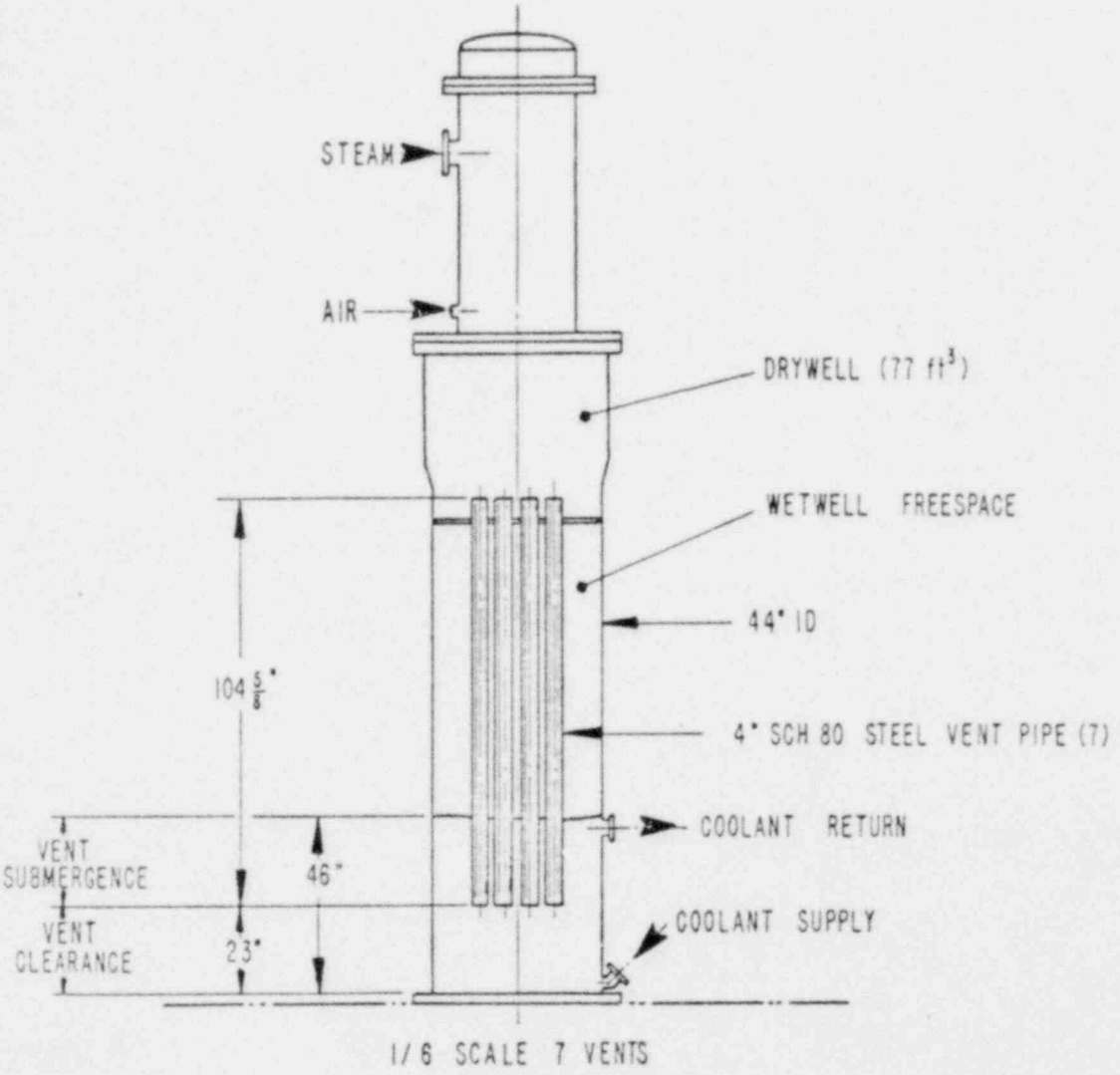

Figure 2-5. Scaled Multivent Test Program - Phase 2 1/6 Scale 7 Vent Geometry

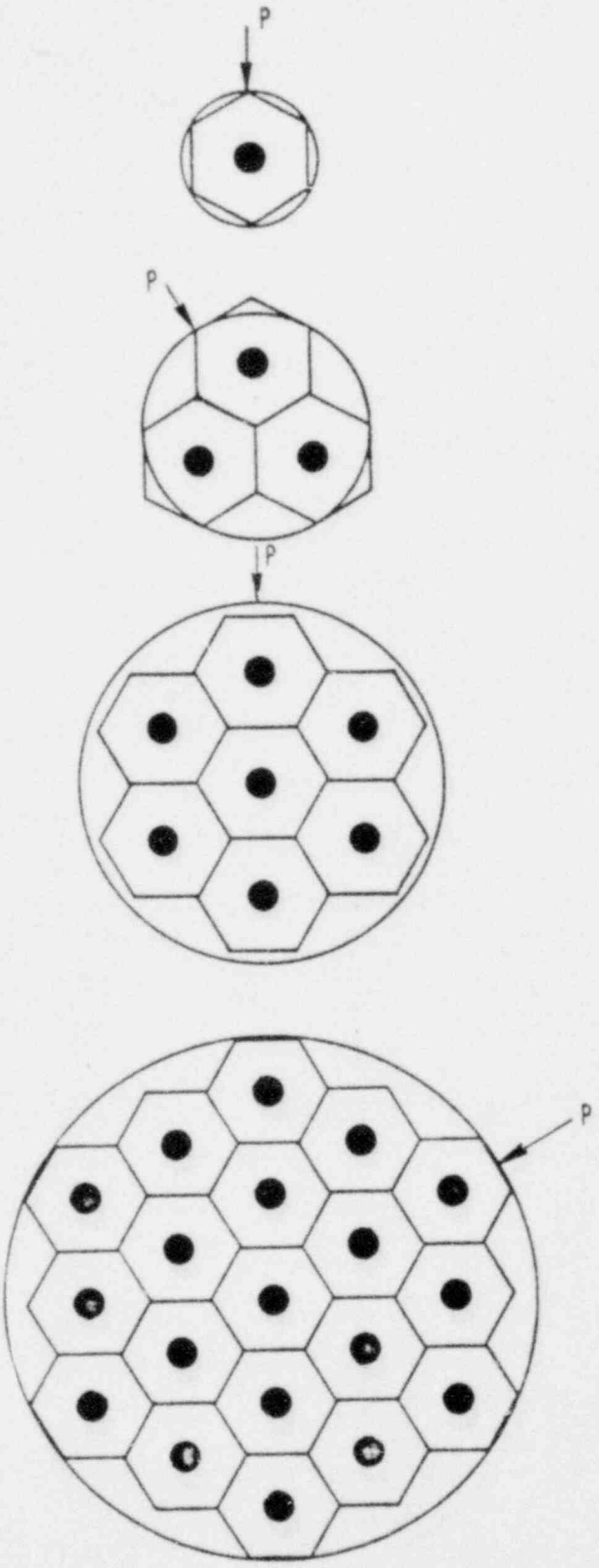

DIMENSIONS	NO OF VENTS			
	1 *	3 *	7 *	19
VENT DIAMETER	2.32"	2.32"	2.32"	2.32"
POOL DIAMETER	10.02"	17.25"	27.25"	44"
POOL TO VENT AREA RATIO	18.6	18.4	19.6	18.9
HEXAGONAL CELL TO POOL AREA RATIO	0.927	0.837	0.783	0.815

P DESIGNATES TYPICAL WALL PRESSURE TRANSDUCER LOCATIONS

* PHASE I GEOMETRIES

Figure 2-6. Scaled Multivent Test Program - Phase 2 1/10 Scale Vent Arrangements

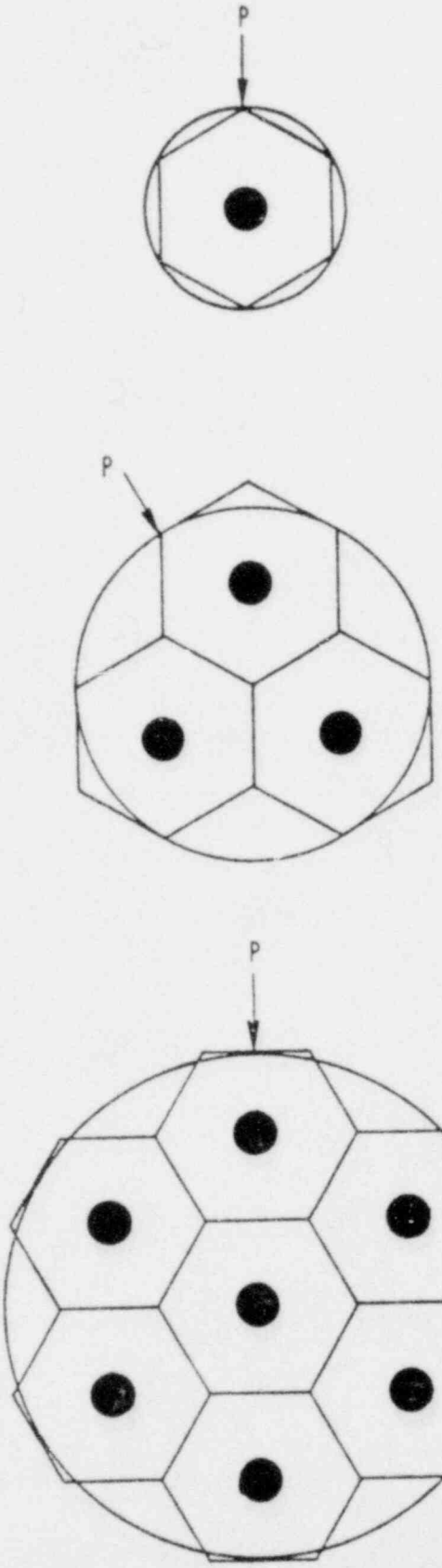

DIMENSIONS	NO OF VENTS		
	1 *	3 *	7
VENT DIAMETER	3.83"	3.83"	3.83"
POOL DIAMETER	17.25"	29.25"	44"
POOL TO VENT AREA RATIO	20.3	19.5	18.9
HEXAGONAL CELL TO POOL AREA RATIO	0.827	0.863	0.89

P DESIGNATES TYPICAL WALL PRESSURE TRANSDUCER LOCATIONS

* PHASE I GEOMETRIES

Figure 2-7. Scaled Multivent Test Program Phase 2 1/6 Scale Vent Arrangements

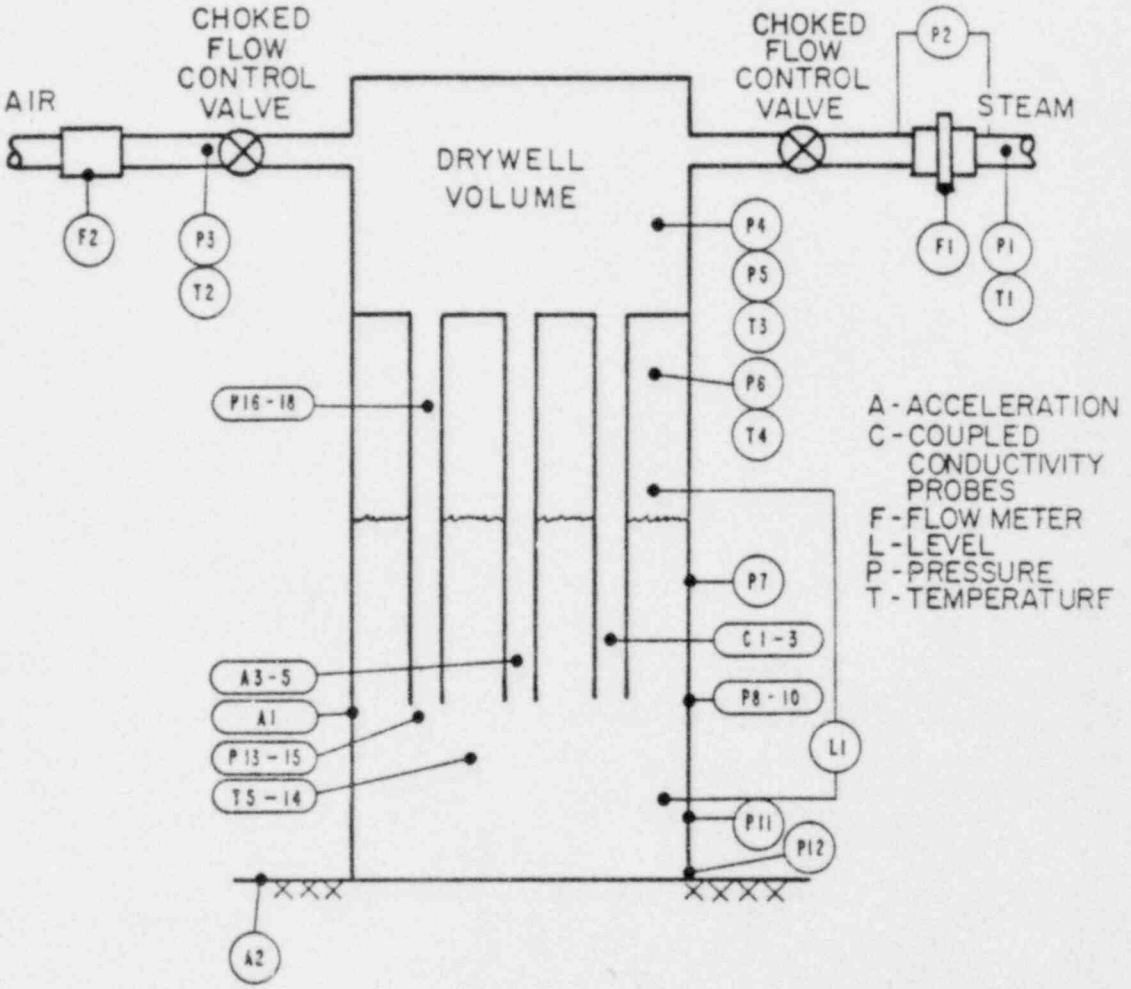

Figure 2-8. Schematic of Instrument Locations (Keyed to Table 2-3)

3. DATA ACQUISITION AND REDUCTION PROCEDURES

In this section data acquisition and reduction procedures are described.

3.1 DATA ACQUISITION SYSTEM AND PROCEDURES

The data acquisition system used for recording the test data is shown in Figure 3-1. The signals from the various instruments were conditioned and amplified to give a ±5 volt full-scale output. The slow response transducer signals listed in Table 3-1 were routed directly via a 64-channel multiplexer to the A/D converter. The fast response transducers listed in Table 3-2 were recorded on a 28-channel FM tape recorder. The reproduce side of the tape recorder was connected to the multiplexer and an oscillograph. The oscillograph output was used for visual monitoring of the data being recorded on the FM tape recorder. Al signals were low-pass filtered prior to data recording consistent with elimination of aliasing during digitization.

The signals from the A/D converter were fed via a microcomputer (DEC LPA11) to a PDP 11/70 minicomputer. After the data were on the PDP 11/70 they could be manipulated and displayed on both video and hardcopy terminals. The low response transducer signals were digitaized at a rate of 15 Hz in real time, that is during the actual test. Key test parameters such as steam mass flux, pool temperature, steam air-content, etc were processed on-line during the test and displayed in engineering units at the data acquisition station. This allowed real time monitoring of the key test parameters. At the start of a typical test, the operator set the required test conditions using analog displays of the system temperatures, pressures and flow rates. The actual test conditions set were monitored using the real time capability of the data acquisition system. After the test parameters were adjusted within specified tolerances a test was initiated.

At the start of the test, a calibration sequence was followed which, starting from zero volts, input a set of known voltages into the signal conditioning/amplifier system (input at the same point as the raw transducer signal). Based on this sequence, the computer automatically obtained the zero offsets and gains

of all the channels and flagged out any malfunctioning channels. After completion of the calibration sequence, test data were recorded for a duration of about 100 seconds. As mentioned earlier, the slow response signals were digitized and input directly to the PDP 11/70, and the fast response channels were recorded on the FM tape recorder. Selected fast response channels were also digitized in real time from the output side of the tape recorder. At the completion of the data recording, time plots and mean values of the key test parameters for the duration of the test were produced. Time plots of the selected fast response channels were also produced to aid in data checking.

3.2 OVERVIEW OF DATA REDUCTION

As described previously, the signals from the slow response channels (listed in Table 3-1) were digitized and input to the PDP 11/70 minicomputer in real time during a test. These channels were digitized at a rate of 15 Hz per channel. This digitization rate was picked because the frequency response of the instruments connected through the slow response channels was less than 5 Hz.

The data from the slow response channels, which consisted mainly of pool temperatures and system data, were reduced to engineering units and the average values over the test duration were stored for data plotting and display purposes.

The fast response channels (listed in Table 3-2), recorded on the FM analog tape recorder, were digitized at a convenient time after the test. The digitization rate for these fast response channels was 10,000 Hz per channel. The fast response channel data were then reduced to give pool wall pressure statistics. Details of the data reduction procedure used for obtaining the statistics is described below.

3.3 WALL PRESSURE DATA REDUCTION

The wall pressure data were reduced to obtain statistics for the peak overpressures (POP), peak underpressures (PUP) and the period between chugs (t_p). Obtaining these statistics involved locating the individual chugs in a given wall pressure trace and then determining the above-mentioned parameters.

A typical chug wall pressure trace is shown in Figure 3-2. The chug begins with an initial underpressure caused by the rapid condensation and the resulting decrease of the pressure inside the steam bubble at the vent exit. This underpressure is usually followed by an overpressure spike caused by the bubble collapse. The pressure spike is in turn followed by oscillations in the pool wall pressures known as the "ringout". This ringout is the response of the pool and the vent to the bubble collapse process. In many conditions (especially at lower steam fluxes) the ringout decays and wall pressure trace goes back to the zero level before the next chug, as shown in Figure 3-2.

A simple algorithm was developed to detect chugs in the pool wall pressure trace and obtain the POP, PUP, and the time at which the POP occurred for each chug. This algorithm works in the following manner. A mean signal level was first computed by averaging the wall pressures over a period τ_a, which was greater than the duration of a chug (see Figure 3-2). A chug was detected when the pressure signal deviated from the mean level by an amount greater than an input threshold - point A in Figure 3-2. After a chug was detected, the maximum and minimum pressures, i.e., the POP and PUP within a specified ringout time window τ_r were obtained. The time at which the POP occurred was also recorded. In the case of the chug shown in Figure 3-2, the POP and PUP would correspond to points B and C, respectively. Note that the PUP is not necessarily the initial underpressure preceding the positive pressure spike.

This algorithm had three operator-specified parameters - the averaging period τ_a, the threshold value and the ringout time window τ_r. The averaging period was selected to be greater than the chug duration and sufficiently long to obtain a good mean signal level. The threshold value was set such that it was 1.5 to 2 times larger than the peak-to-peak value of the noise. The ringout window was chosen by examining the wall pressure trace and determining the time between the initial depressurization and the point where the ringout decayed to below the threshold value.

The normal procedure followed in using this algorithm was to first examine the wall pressure trace and choose the three above-mentioned parameters. The algorithm was then run on several seconds of the pressure data to check (visually

on a video terminal) that the values of the parameters chosen did indeed result in the successful detection of all the chugs present in that duration. If the results were positive, the chug finding algorithm was then run for the entire duration of the test or until 300 chugs were detected, whichever occurred first.

This algorithm was only run on the pool bottom elevation pressure trace, and the time of occurrence of the POP as well as the magnitude of the POP and PUP for individual chugs were recorded. From these, the mean values and standard deviations for the POP, PUP and t_p (time interval between successive POPs) were computed.

In the other five pool wall pressure traces, POP, PUP and the time of occurrence of the POP were obtained by scanning only those portions of the trace which corresponded to the time window within which a chug was found to occur at the wall bottom location. Using this procedure considerably reduced the time required to process these other pool wall pressure traces.

The pattern of the "classic" chug is illustrated in Figure 3-3. Here, at the start of the chug, the vent is dry and both pool and vent static pressure decrease. This is caused by the rapid condensation occurring at the vent exit which reduces the pressure in the steam bubble and induces an increased steam flow in the vent which, in turn, reduces the vent static pressure. The bubble collapse produces the spike in the wall pressure trace. At some point, the condensation at the vent exit is reduced drastically causing a positive pressure wave to propagate up the vent causing the vent static pressure to increase. From then on, both the pool and vent ring at their respective natural frequencies. Due to the impedance mismatch at the steam water interface, the vent rings at its natural frequency whereas the pool wall pressure ringout contains components from both the pool and vent ringout. The character of the pool wall pressure signal does not always follow that of the "classic" chug, however. In some tests, the pool wall pressure signal shows an almost continuous oscillation at or near the vent acoustic frequency, as seen in Figure 3-4. In this case there is no water entry into the vent following the chug and the pool and vent pressure traces have the same general pattern. This behavior was noted in Phase I (see Reference 1) and was even more evident in the Phase 2 data, especially for the larger vent sizes at low subcooling and high steam mass flux.

The chug-finding algorithm was applied to all the data in Phase 2, both classical chugging and the oscillating type. In the latter type, the mean POP, PUP and chug period are much more sensitive to the threshold and ringout period than for classical chugging. The results of the computerized chug-finding routine were checked for each test to ensure that the correct threshold and ringout had been applied.

Table 3-1

SLOW RESPONSE CHANNELS* INPUT DIRECTLY TO COMPUTER

Instrument	Direct LPA Channel	Instrument	Direct LPA Channel
Air Pressure	28	Mid-Submergence 4 Temperature	48
Wetwell Pressure**	29	Mid-Submergence 5 Temperature	49
Steam Supply Pressure	30	Pool Top Temperature	50
Drywell Pressure	31	Steam Supply 1 Temperature	51
Water Flow Rate	34	Steam Supply 2 Temperature	52
Steam Flow Rate**	35	Remote Steam Supply Temperature	53
Pool Level**	37	Coolant Inflow Temperature	54
Pool Bottom Temperature	38	Coolant Outflow Temperature	55
Mid-Clearance Temperature	39	Wetwell Airspace Pressure	56
Exit Elevation 1 Temperature	40	Drywell Temperature	57
Exit Elevation 2 Temperature	41	Mid-Submergence 3 Temperature**	58
Exit Elevation 3 Temperature	42	Remote Steam Flow Rate	59
Exit Elevation 4 Temperature	43	Remote Steam Pressure	60
Exit Elevation 5 Temperature	44	Master Reference Voltage	61
Mid-Submergence 1 Temperature	45	Air Flow Rate	62
Mid-Submergence 2 Temperature	46	Air Supply Temperature	63

*Signal conditioning amplifiers band-limited from DC to 3 Hz.
**Also recorded on analog magnetic tape.

Table 3-2

FAST RESPONSE CHANNELS* RECORDED ON ANALOG TAPE

Instrument	LPA Channel (from tape reproduce side)	Tape Channel	Instrument	LPA Channel (from tape reproduce side)	Tape Channel
Bottom Wall Pressure	[0]	16	Vent 1 Level	[13]	13
Vent 1 Static Pressure	[1]	1	Vent 2 Level	[14]	14
Vent 2 Static Pressure	[2]	2	Vent 3 Level	[15]	15
Vent 3 Static Pressure	[3]	3	Vent Wall Acceleration	[19]	18
Vent 1 Source Pressure	[4]	4	Baseplate Acceleration	[20]	19
Vent 2 Source Pressure	[5]	5	Fast Wetwell Pressure	[18]	17
Vent 3 Source Pressure	[6]	6	Vent 1 Acceleration	[21]	20
Vent 1 Wall Pressure	[7]	7	Vent 2 Acceleration	[25]	21
Vent 2 Wall Pressure	[8]	8	Vent 3 Acceleration	[26]	22
Vent 3 Wall Pressure	[9]	9	Slow Wetwell Pressure**	[32]	24
Mid-Submergence Wall Pressure	[10]	10	Steam Flow Rate**	[33]	25
			Pool Level**	[36]	26
Mid-Clearance Wall Pressure	[11]	11	Mid-Submergence 3 Temperature	[47]	27
Fast Drywell Pressure	[12]	12			

*Signal conditioning amplifiers band limited from DC to 3 kHz.

**These low response channels also recorded digitally and band limited from DC to 3 Hz.

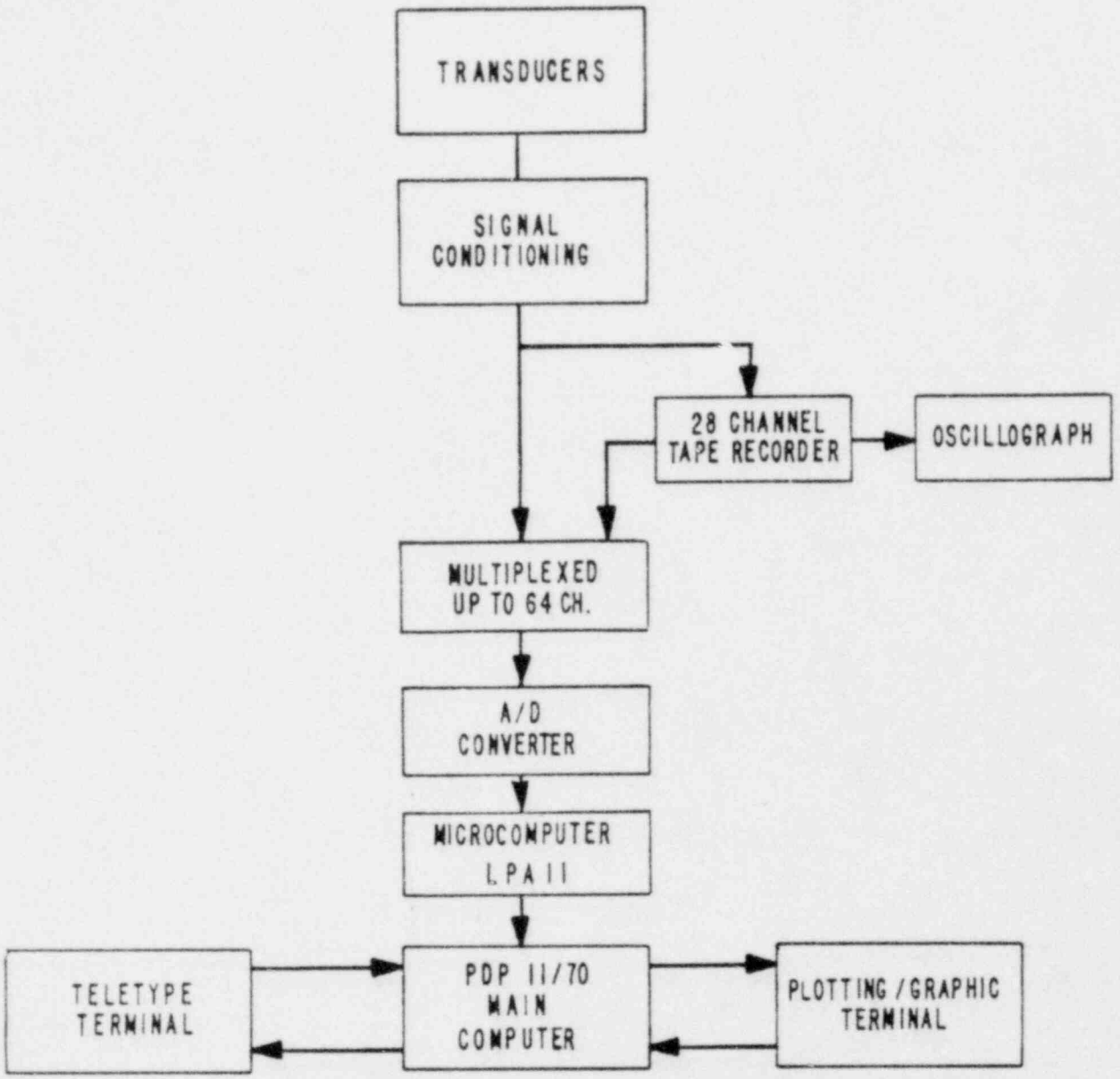

Figure 3-1. Schematic of the Data Acquisition System

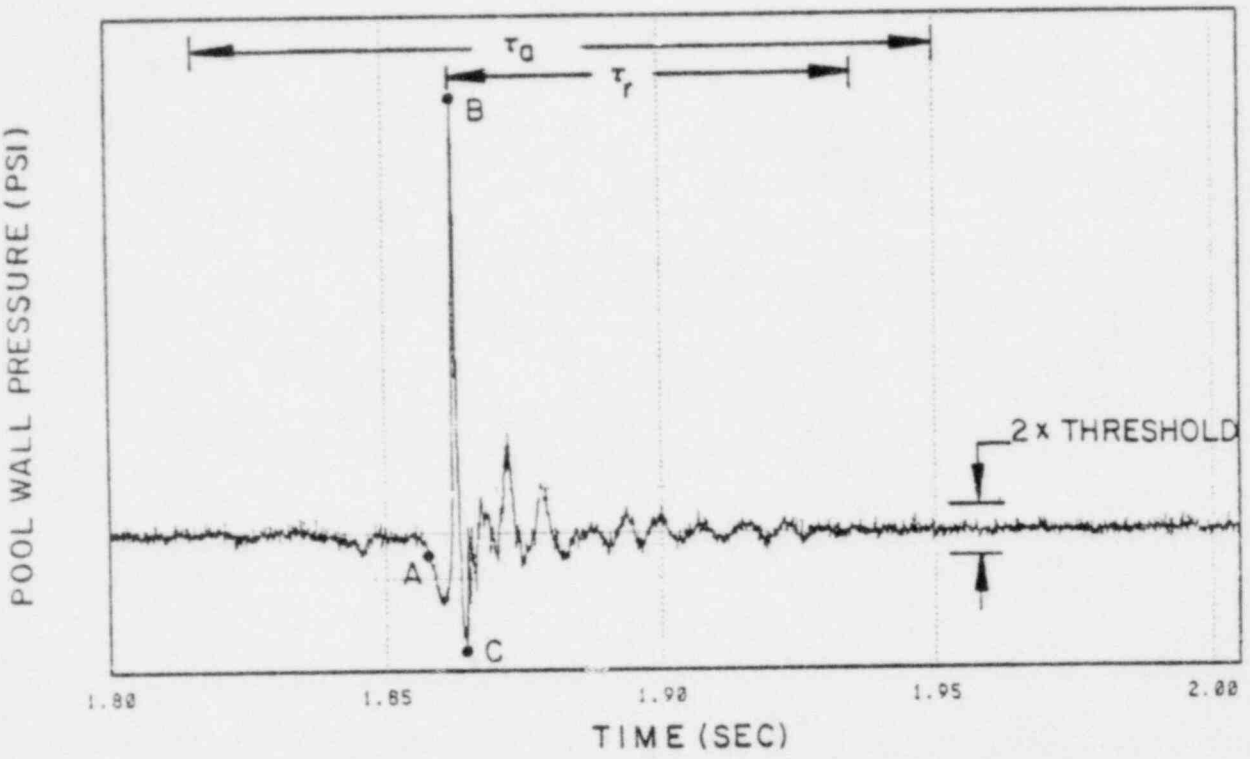

Figure 3-2. Typical Time Windows and Threshold Used by the Chug Finding Algorithm

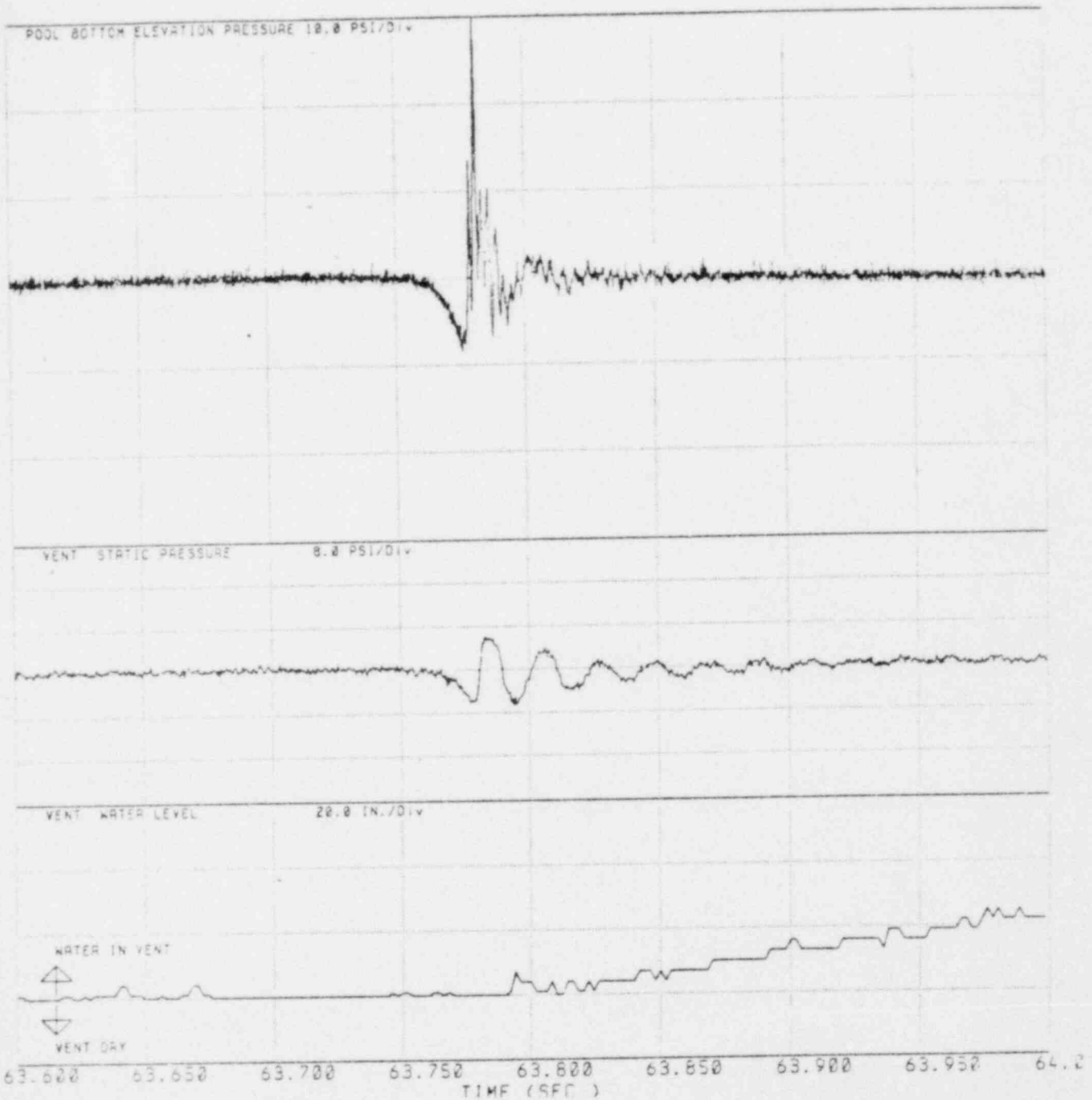

Figure 3-3. A Classical Chug in a Single Vent Geometry

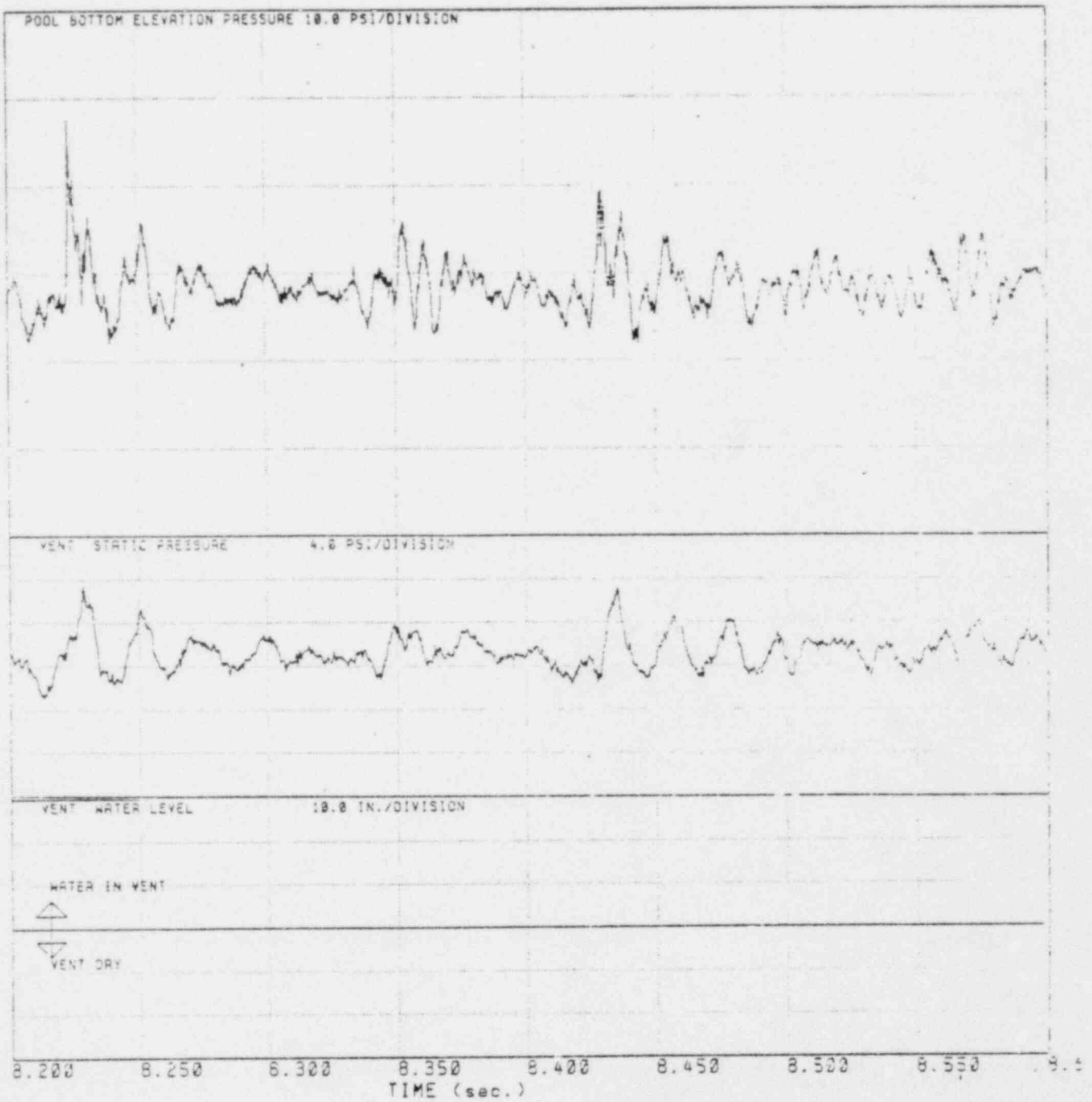

Figure 3-4. Oscillatory Chug in a Single Vent Geometry

4. TEST MATRIX

The test matrix used for the Phase 1 baseline geometries (1, 3, and 7 vents at 1/10 scale and 1 and 3 vents at 1/6 scale) and the five Phase 2 geometries is shown in Table 4-1. Limitation of the steam supply set the maximum steam mass flux for the Phase 2 geometries to 10 lbm/sec-ft^2, except the 1/4-scale single vent geometry.

The test conditions were chosen based on the requirements of two scaling approaches, Mach scaling and Froude scaling, as discussed in Reference 4. These approaches result from choosing different sets of parameters to non-dimensionalize the system of equations governing the motion of the steam and water during chugging.

Since no single scaling approach will satisfy all aspects of the chugging phenomenon, the test matrices were made sufficiently broad to cover a wide range of flow and thermal conditions. With the single vent tests performed over a wide range of scales in the Scaled Multivent Test Program, this strategy provided sufficient data to evaluate the effects of scale on the chugging phenomenon and demonstrate the applicability of the subscale multi-vent effects to full-scale.

The data comparisons which can be made among the Phase 1 and Phase 2 geometries are displayed in Table 4-2. Geometries A, K, P and U provided the 1/10 scale data at 1, 3, 7 and 19 vents, respectively. Geometries J, M and V provided the 1/6 scale data for 1, 3, and 7 vents. Single vent data at four scales were obtained from geometries A, J, T and S. The data on the effect of vent length on chugging were obtained from geometries R and S.

Table 4-1

TEST MATRIX FOR PHASE 1 AND PHASE 2
GEOMETRIES* 1, 9, 10, 12, 14, 15, 16, 17, 18, 19*

Pressure (psia)	Froude Scaled†		14.7	45	
Steam Mass Flux ($lbm/sec\text{-}ft^2$)	0.1,0.2 0.5,1,2	0.1,0.5, 2	0.2,1, 4	0.5,1,2,4, 8,10**,16***	1,4,10** 16***
Air Content (%)	0	0.1,0.2, 0.5	0	0	0.1,0.2, 0.5
Temperature (°F)	90, 130	90	90,130	90,130, 160,200	130
Number of Tests	100	90	60	244	93

Total Number of Tests: 587

†Froude scaled pressure is obtained by multiplying the full-scale pressure (45 psia) by the scale factor.
*See Reference 1 and Table 2-1 for description of test geometries.
**Steam mass flux of 10 $lbm/sec\text{-}ft^2$ for Geometries 15, 16, 17, 18, 19.
***Steam mass flux of 16 $lbm/sec\text{-}ft^2$ for Geometries 1, 9, 10, 12, 14, 17.

Table 4-2

PHASE 1 AND PHASE 2 DATA COMPARISONS

Geometries*	Purpose
A, K, L, U	Baseline 1/10 scale single and multivent data
J, M, V	Baseline 1/6 scale single and multivent data.
A, J, T, S	Effect of scale on single vent chugging.
R, S	Effect of vent length at 5/12 scale.

*See Reference 1 and Table 2-1 for geometry descriptions.

5. TEST RESULTS AND DISCUSSION ON SINGLE VENT DATA AT FOUR SCALES

The data from the 1/4 and 5/12 single vent geometries along with data from the Phase 1 1/10 and 1/6 scale single vent geometries are discussed in Subsections 5.1 through 5.3 in terms of the effect on chugging of the thermodynamic parameters—steam mass flux, pool temperature and steam air content. The 5/12 single vent data for the effect of vent length on chugging are presented in Section 5.4

The data in the following Subsections are for tests at a wetwell airspace pressure of 45 psia ("Mach scaled"). The data are presented in terms of the mean peak overpressure (POP), mean peak underpressure (PUP) and chug frequency (inverse of the mean period between chugs t_p). The mean values are defined as the average of all values of the parameter found in a test run using the chug-finding algorithm discussed in Subsection 3.3.

Pool wall pressure measurements were made at six locations for each test geometry, but only data from the pool wall bottom elevation are reported. The maximum pool boundary value of POP is observed at this location (see Reference 1) and pressures at other locations are related to it in a fairly constant fashion. Hence, trends at all other wall pressure measurement locations will be similar to those for the pool bottom location.

The control of test conditions such as steam mass flux, air content of the steam, pool temperature, pool level and freespace pressure was very good, and generally well within the tolerances given in Table 2-3. The actual ranges of these parameters are given on each data plot.

Although chugging at the two larger scales (1/4 and 5/12 scales) is similar to that in 1/10 and 1/6 scales, there are some differences due to scale in the trends of mean POP, PUP and chug frequency with the various test parameters. These differences will be pointed out when the appear in the data plots, but explanations for the cause of such variations will be reserved for the final report.

5.1 EFFECT OF STEAM MASS FLUX

The effect of steam mass flux on single vent chugging at four scales is presented in this Subsection. Steam mass flux is one of the most important test parameters and affects both the amplitude and frequency of chugging. Figures 5-1 through 5-7 are traces of the pool wall pressure, vent static pressure, drywell pressure and vent water level for the 1/4 scale vent at several steam mass fluxes, 45 psia wetwell airspace pressure, 130°F pool temperature and zero steam air-content.

At a steam mass flux of 0.5 lbm/sec-ft^2 the chugs are of low amplitude with the water completely clearing the vent before the next chug occurs (Figure 5-1). As the steam mass flux is increased to 4 lbm/sec-ft^2, the amplitude of the chug increases, as do the vent and drywell pressure fluctuations (Figures 5-2, 5-3 and 5-4). Occasionally a rapid condensation event occurs while water is still in the vent (at approximately 47.35 seconds in Figure 5-2 and 12.8 seconds in Figure 5-4, for example). However, such an occurrence does not result in very significant pressure fluctuations at the pool wall.

At steam mass flux values above 8 lbm/sec-ft^2 the chug amplitude does not increase markedly, and the signal at the wall becomes interspersed with periods of fairly regular oscillations at the vent acoustic frequency of 45 Hz (Figures 5-5, 5-6 and 5-7). Also, during these periods of regular oscillation there is usually no water reentry into the vent, indicating that the steam-water interface oscillates near the vent exit.

The variations in mean POP, PUP and chug frequency with steam mass flux are displayed* in Figures 5-8, 5-9 and 5-10 at a pool temperature of 130°F and in Figures 5-11, 5-12 and 5-13 at a pool temperature of 160°F. The data trends shown in these figures are similar for all four scales.

---

*The 5/12-scale data are for the standard vent length – Geometry S.

In the two smaller scales, the trend in POP shows a slight flattening as the mass flux increases from 2 to 4 lbm/sec-ft^2. This behavior is more pronounced at the larger scales and both the 1/4 and 5/12 scale vents show a distinct reduction in the POP at about 2 to 4 lbm/sec-ft^2, followed by a rise as the steam flux is further increased. This reduction in pool wall pressure coincides with a change in the character of the condensation process at the vent exit from discrete chugging to the more oscillatory behavior mentioned earlier. Figures 5-14 and 5-15 are composites of the pool wall pressure for the 5/12 scale vent over a range of steam mass flux values at pool temperatures of 130°F and 160°F. Both figures clearly show this transition.

Chug frequency increases with steam mass flux for all four scales.

The trends in mean POP, PUP and chug frequency with steam mass flux at pool temperatures of 90°F and 200°F are similar to those displayed here.

5.2 EFFECT OF POOL TEMPERATURE

5.2.1 Pool Temperature Distribution

The nominal pool temperature was defined as the temperature measured at the mid-submergence elevation and at a radial location of $r/D_w = 0.37$, where r is the radial position of the probe measured from the center of the wetwell and D_w is the wetwell diameter. For the single vent geometries, there were 11 other temperature measurement locations which were used to determine the depth-wise and circumferential temperature distributions within the pool.

As described in Subsection 2.1 in a given test a fixed pool temperature was maintained by circulating coolant water through the pool. Under all test conditions the circumferential distributions of temperature were uniform (measured at the vent exit and mid-submergence elevations). This uniformity indicates that the number and locations of water supply and distribution points were adequate and did not result in any measurable flow distortions in the pool.

The pool temperture profiles for the 1/4 scale single vent are shown in Figures 5-16 and 5-17 at nominal pool temperatures of 90°F and 160°F for several steam mass flux values. As shown, the distributions are uniform except that the bottom of the pool tends to be slightly cooler than at the higher elevations at low steam mass flux and higher pool temperature. At 5/12 scale (Figures 5-18 and 5-19) there is considerable depthwise stratification in the pool, even at higher mass flows. For example, at 4 lbm/sec-ft^2 and a nominal pool temperature of 160°F, the temperature at pool bottom and up to the mid-clearance elevation is essentially at the coolant supply temperature. The degree of stratification is reduced as the steam mass flux is increased indicating an improvement in the pool mixing due to normal chugging. This observation of pool stratification is consistent with the transition to the oscillatory chug behavior discussed in Subsection 5.1.

5.2.2 Effects of Pool Temperature

The effect of pool temperature on mean POP for the single vent geometries at several steam mass fluxes is shown in Figures 5-20 through 5-23. In general, the data trends are similar at all four scales with the magnitude of the mean POP decreasing with increasing scale. It is seen that for steam mass flux $\leq$ 8 lbm/sec-ft^2, the mean POP reaches a maximum in the 130°F to 170°F pool temperature range. In the 16 lbm/sec-ft^2 steam mass flux (Figure 5-23), the mean POP shows a continuous increase with increasing pool temperature. Finally, regardless of the steam mass flux, the mean POP is expected to decrease as the pool temperature approaches the saturation temperature.

The effect of pool temperature on mean PUP is shown in Figures 5-24 through 5-27 for the four single vent geometries. Again, the data trends are similar at all scales, with the mean PUP decreasing with increasing pool temperature at steam mass fluxes $\leq$ 8 lbm/sec-ft^2. However, at the higher steam mass fluxes, mean PUP remains nearly constant over the range of pool temperatures tested.

Pool temperature does not have a significant effect on chug frequency for the single vent geometries (Figures 5-28 through 5-31) at any steam mass flux, although there is a slight trend to a maximum in chug frequnecy in the range of 100°F to 150°F for the higher mass fluxes.

The effect of pool temperature on chugging for the 1/4 scale single vent at a mass flux of 4 lbm/sec-ft^2 is shown clearly in Figures 5-32 through 5-35 and at 16 lbm/sec-ft^2 in Figures 5-36 through 5-39. At the lower mass flux the chug amplitude reaches a maximum at 130°F pool temperature. Also, the drywell and vent pressure fluxtuations and the water reentry into the vent are maximum at this temperature for the 4 lbm/sec-ft^2 steam flux. At a steam mass flux of 16 lbm/sec-ft^2 the pool bottom pressure signal keeps increasing to the maximum temperature, consistent with the trend in mean POP (Figure 5-23). At the 90°F pool temperature (Figure 5-36) drywell depressurizations are somewhat erratic and the vent static pressure shows an almost continuous oscillation at vent acoustic frequency. As the temperature increases the drywell pressure fluctuations become more regular with a larger amplitude indicating a strong, rapid condensation at the vent exit.

In summary, pool temperature influences chugging in a similar way for the single vents at four scales. At steam mass fluxes $\leq$ 8 lbm/sec-ft^2 the mean POP shows a maximum at a pool temperature of about 130°F to 150°F followed by a decrease as the pool temperature approaches saturation. At a steam mass flux of 16 lbm/sec-ft^2 for the three smaller vents, the POP shows a continuous increase up to the maximum pool temperature tested. Mean PUP generally decreases with pool temperature at all scales for steam mass fluxes $\leq$ 8 lbm/sec-ft^2, independent of pool temperature at higher steam mass fluxes. Pool temperature has little effect on chug frequency.

5.3 EFFECT OF STEAM AIR CONTENT

The baseline chugging data were obtained using steam having negligible amounts of air or other non-condensibles (estimated to be less than 20 ppm). To study the effect of non-condensibles in the steam on chugging, tests were run at several steam fluxes with steam air-content up to 0.5% by mass at a

pool temperature of 130°F and at 45 psia wetwell airspace pressure. Figures 5-40 through 5-45 show the mean POP, PUP and chug frequency data for the single vent geometries at steam mass flux values of 4 and 16 lbm/sec-ft^2 (only the three smaller scales were tested at the higher steam mass flux).

As expected, mean POP and PUP decrease with increasing steam air content at constant steam mass flux and pool temperature. At the lower steam mass flux of 4 lbm/sec-ft^2 there does not appear to be an obvious trend in chug frequency with steam air-content (Figure 5-42) whereas at 16 lbm/sec-ft^2 the chug frequency shows a decrease with increasing air content (Figure 5-45).

Data traces for the 1/4 scale vent at a steam mass flux of 4 lbm/sec-ft^2 and over the range of steam air-content are shown in Figures 5-46 through 5-49. The introduction of a small amount of air (0.1% by mass) changes the pool bottom pressure signal from chugging to a pronounced oscillatory behavior, and also reduces the amplitude of the rapid condensation as evidenced in the vent static and drywell pressure traces (Figures 5-46 and 5-47). Further increases in air content result in continued reduction of pool wall pressure amplitude, but the character of the signal remains the same. At the highest air content (Figure 5-49) the drywell pressure fluctuations are quite small and there is no water reentry to the vent.

These results are in agreement with those seen in other single vent chugging tests (see Reference 1 and 7).

5.4 EFFECT OF VENT LENGTH

In the baseline single and multiple vent geometries of Phase 1 and Phase 2, the vent length was maintained at approximately 9-ft. This length provided the greatest utilization of the test vessels for assembling the different vent geometries. One geometry in Phase 2 at 5/12 scale was selected to provide data for evaluating the effect of vent length on chugging.

In this subsection the results from the 5/12 scale geometry with a 17-ft vent length (Geometry R) are compared with those for the 5/12 scale geometry with the 9.7-ft vent length (Geometry S). Plots of mean POP, PUP and chug frequency as a function of steam mass flux, pool temperature and air content are used to show the effect of the increased vent length. In addition, data traces of the pool wall bottom elevation pressure, vent static pressure and drywell pressure for these geometries are presented.

Figures 5-50, 5-51 and 5-52 show the mean POP, PUP and chug frequency data as a function of steam mass flux for the two vent lengths at 130°F pool temperature and zero steam air-content. The trends in POP and PUP are similar; both vents exhibit a peak in chug amplitude at about 1 to 2 lbm/sec-ft^2 steam mass flux, followed by a decrease at 4 lbm/sec-ft^2. As discussed in the previous section, this decrease in the mean POP and PUP at 4 lbm/sec-ft^2 is due to a transition from classical chugging at 1 to 2 lbm/sec-ft^2 to an oscillatory type chugging at 4 lbm/sec-ft^2.

For the longer vent, the mean POP and PUP remain nearly constant at the higher steam mass fluxes of 8 and 10 lbm/sec-ft^2. However, for the shorter vent, both the mean POP and PUP increased markedly at 10 lbm/sec-ft^2 steam flux. As shown later, the difference in the behavior of mean POP and PUP is due to the fact that the shorter vent reverts to classical chugging as the steam mass flux is increased from 8 to 10 lbm/sec-ft^2. Whereas the longer vent continues to exhibit oscillatory chugs at 10 lbm/sec-ft^2 steam mass flux.

The mean chug frequency for the shorter vent shows an increase with increasing steam mass flux. Such a monotonic trend is not observed at the longer vent.

The effect of pool temperature on mean POP, PUP and frequency at a steam mass flux of 4 lbm/sec-ft^2 are shown in Figures 5-53, 5-54, and 5-55. The effect of pool temperature is shown as being similar for both vent lengths. This was found to be true at all steam mass fluxes whre the nature of chugging (classical type or oscillatory type) was similar for both vent lengths.

However, at 10 lbm/sec-ft^2 where the shorter vent shows classical chugging and the longer vent shows oscillatory chugging, the effect of pool temperature on mean POP and PUP is markedly different as seen from Figures 5-56 and 5-57. For the longer vent, the mean POP and PUP remain nearly constant over the range of pool temperatures tested. On the other hand, the mean POP for the shorter ventpeaks at 130°F followed by a continued increase with further increase in pool temperature. The mean PUP for the shorter vent shows a similar behavior. Pool temperature does not have a significant effect on the chug frequency (Figure 5-58) at this steam flux for the short and long vents.

The effects of steam air content on mean POP, PUP, and chug frequency for the two vent lengths at a steam mass flux of 10 lbm/sec-ft^2 and 130°F pool temperature are shown in Figures 5-59, 5-60 and 5-61. Both POP and PUP decrease with increasing steam air content for both vents, with the effect being more pronounced for the short vent for this mass flux. Steam air content does not have a marked effect on chug frequency, and there is no obvious difference in the values of chug frequency for the two vent lengths.

The most significant characteristic of the longer vent was a greater tendency towards oscillatory type chugging compared with the shorter vent. For instance, Figure 5-62 and 5-63 compare the data traces for the long and short vents at a pool temperature of 160°F and steam mass flux of 2 lbm/sec-ft^2 and Figures 5-64 and 5-65 make the same comparison at 160°F and 10 lbm/sec-ft^2. For each set of thermodynamic parameters, the long vent has very strong, regular oscillations at its acoustic frequency (approximately 25 Hz), whereas the shorter vent shows chugging with ringout at its acoustic frequency (about 45 Hz).

Further evidence of this oscillatory behavior for the longer vent is seen in the pool temperature profile plots of Figures 5-66 and 5-67. Here, for the long vent the vertical stratification is more pronounced over a wide range of steam flux values than is the case for the shorter vent. At 10 lbm/sec-ft^2 steam flux, for example, the temperature at the pool bottom for the long vent (Figure 5-66) is about 10°F higher than the coolant supply temperature,

whereas for the short vent the temperature at pool bottom is 60°F higher than the supply temperature (Figure 5-67). This increased temperature rise at the pool bottom is indicative of the higher degree of pool mixing which is obtained from the chugging behavior of the short vent versus the more oscillatory behavior of the long vent.

That this oscillatory behavior is not isolated to a single pool temperature or steam mass flux is shown by the next set of data traces and pool temperature profile data. Figures 5-68 and 5-69 compare the pool wall bottom elevation pressure, vent static pressure and drywell pressure traces for the long and short vents at a steam mass flux of 8 lbm/sec-ft^2 and 130°F pool temperature. Figures 5-70 and 5-71 show the corresponding pool temperature profile data. Again, the long vent shows oscillatory pressure traces on the pool wall and in the vent, and exhibits a greater temperature stratification in the pool.

In summary, increased vent length at 5/12 scale tends to provide chugging of a more oscillatory nature than in the case of the short vent. The trends in mean POP, PUP and chug frequency with the thermodynamic parameters are generally similar between the two vent lengths. The magnitude of the POP, PUP and chug frequency is slightly greater for the short vent than for the long vent at the same thermodynamic conditions.

The following Figures are GENERAL ELECTRIC COMPANY PROPRIETARY and have been removed from this document in their entirety.

Figure 5-1 Data Traces at 0.5 lbm/sec-ft^2 Steam Mass Flux - 1/4 Scale Single Vent Tests

Figure 5-2 Data Traces at 1.0 lbm/sec-ft^2 Steam Mass Flux - 1/4 Scale Single Vent Tests

Figure 5-3 Data Traces at 2.0 lbm/sec-ft^2 Steam Mass Flux - 1/4 Scale Single Vent Tests

Figure 5-4 Data Traces at 4.0 lbm/sec-ft^2 Steam Mass Flux - 1/4 Scale Single Vent Tests

Figure 5-5 Data Traces at 8.0 lbm/sec-ft^2 Steam Mass Flux - 1/4 Scale Single Vent Tests

Figure 5-6 Data Traces at 10.0 lbm/sec-ft^2 Steam Mass Flux - 1/4 Scale Single Vent Tests

Figure 5-7 Data Traces at 16.0 lbm/sec-ft^2 Steam Mass Flux - 1/4 Scale Single Vent Tests

Figure 5-8 Variation of Mean POP at Pool Bottom Elevation with Steam Mass Flux and 130°F Pool Temperature - Single Vent Tests at Four Scales

Figure 5-9 Variation of Mean PUP at Pool Bottom Elevation with Steam Mass Flux and 130°F Pool Temperature - Single Vent Tests at Four Scales

Figure 5-10 Variation of Mean Chug Frequency with Steam Mass Flux and 130°F Pool Temperature - Single Vent Tests at Four Scales

Figure 5-11 Variation of Mean POP at Pool Bottom Elevation with Steam Mass FLux and 160°F Pool Temperature - Single Vent Tests at Four Scales

Figure 5-12 Variation of Mean PUP at Pool Bottom Elevation with Steam Mass Flux and 160°F Pool Temperature - Single Vent Tests at Four Scales

Figure 5-13 Variation of Mean Chug Frequency with Steam Mass Flux and 160°F Pool Temperature - Single Vent Tests at Four Scales

Figure 5-14 Pool Bottom Elevation Pressure Traces at 130°F Pool Temperature and Five Steam Mass Fluxes - 5/12 Scale Single Vent Tests

The following Figures are GENERAL ELECTRIC COMPANY PROPRIETARY and have been removed from this document in their entirety.

Figure 5-15 Pool Bottom Elevation Pressure Traces at 160°F Pool Temperature and Five Steam Mass Fluxes - 5/12 Scale Single Vent Tests

Figure 5-16 Pool Temperature Distribution at Various Steam Mass Fluxes and 90°F Pool Temperature - 1/4 Scale Single Vent Tests

Figure 5-17 Pool Temperature Distribution at Various Steam Mass Fluxes and 160°F Pool Temperature - 1/4 Scale Single Vent Tests

Figure 5-18 Pool Temperature Distribution at Various Steam Mass Fluxes and 90°F Pool Temperature - 5/12 Scale Single Vent Tests

Figure 5-19 Pool Temperature Distribution at Various Steam Mass Fluxes and 160°F Pool Temperature - 5/12 Scale Single Vent Tests

Figure 5-20 Variation of Mean POP at Pool Bottom Elevation with Pool Temperature and 4 lbm/sec-ft^2 Steam Mass Flux - Single Vent Tests at Four Scales

Figure 5-21 Variation of Mean POP at Pool Bottom Elevation with Pool Temperature and 8 lbm/sec-ft^2 Steam Mass Flux - Single Vent Tests at Four Scales

Figure 5-22 Variationof Mean POP at Pool Bottom Elevation with Pool Temperature and 10 lbm/sec-ft^2 Steam Mass Flux - Single Vent Tests at Two Scales

Figure 5-23 Variation of Mean POP at Pool Bottom Elevation with Pool Temperature and 16 lbm/sec-ft^2 Steam Mass Flux - Single Vent Tests at Three Scales

Figure 5-24 Variation of Mean PUP at Pool Bottom Elevation with Pool Temperature and 4 lbm/sec-ft^2 Steam Mass Flux Single Vent Tests at Four Scales

Figure 5-25 Variation of Mean PUP at Pool Bottom Elevation with Pool Temperature and 8 lbm/sec-ft^2 Steam Mass Flux Single Vent Tests at Two Scales

Figure 5-26 Variation of Mean PUP at Pool Bottom Elevation with Pool Temperture and 10 lbm/sec-ft^2 Steam Mass Flux Single Vent Tests at Two Scales

The following Figures are GENERAL ELECTRIC COMPANY PROPRIETARY and have been removed from this document in their entirety.

Figure 5-27 Variation of Mean PUP at Pool Bottom Elevation with Pool Temperature and 16 lbm/sec-ft^2 Steam Mass Flux - Single Vent Tests at Three Scales

Figure 5-28 Variation of Mean Chug Frequency with Pool Temperature and 4 lbm/sec-ft^2 Steam Mass Flux - Single Vent Tests at Four Scales

Figure 5-29 Variation of Mean Chug Frequency with Pool Temperature and 8 lbm/sec-ft^2 Steam Mass Flux - Single Vent Tests at Four Scales

Figure 5-30 Variation of Mean Chug Frequency with Pool Temperature and 10 lbm/sec-ft^2 Steam Mass Flux = Single Vent Tests at Two Scales

Figure 5-31 Variation of Mean Chug Frequency with Pool Temperature and 16 lbm/sec-ft^2 Steam Mass Flux - Single Vent Tests at Three Scales

Figure 5-32 Data Traces at 90°F Pool Temperature and 4 lbm/sec-ft^2 Steam Mass Flux - 1/4 Scale Single Vent Tests

Figure 5-33 Data Traces at 130°F Pool Temperature and 4 lbm/sec-ft^2 Steam Mass Flux - 1/4 Scale Single Vent Tests

Figure 5-34 Data Traces at 160°F Pool Temperature and 4 lbm/sec-ft^2 Steam Mass Flux - 1/4 Scale Single Vent Tests

Figure 5-35 Data Traces at 200°F Pool Temperature and 4 lbm/sec-ft^2 Steam Mass Flux - 1/4 Scale Single vent Tests

Figure 5-36 Data Traces at 90°F Pool Temperature and 16 lbm/sec-ft^2 Steam Mass Flux - 1/4 Scale Single Vent Tests

Figure 5-37 Data Traces at 130°F Pool Temperature and 16 lbm/sec-ft^2 Steam Mass Flux - 1/4 Scale Single Vent Tests

Figure 5-38 Data Traces at 160°F Pool Temperature and 16 lbm/sec-ft^2 Steam Mass Flux - 1/4 Scale Single Vent Tests

Figure 5-39 Data Traces at 2000°F Pool Temperature and 16 lbm/sec-ft^2 Steam Mass Flux - 1/4 Scale Single Vent Tests

Figure 5-40 Variation of Mean POP at Bottom Elevation with Steam Air Content and 4 lbm/sec-ft^2 Steam Mass FLux - Single Vent Tests at Four Scales

The following Figures are GENERAL ELECTRIC COMPANY PROPRIETARY and have been removed from this document in their entirety.

Figure 5-41 Variation of Mean PUP at Pool Bottom Elevation with Steam Air Content and 4 lbm/sec-ft^2 Steam Mass Flux - Single Vent Tests at Four Scales

Figure 5-42 Variation of Mean Chug Frequency with Steam Air Content and 4 lbm/sec-ft^2 Steam Mass Flux - Single Vent Tests at Four Scales

Figure 5-43 Variation of Mean POP at Pool Bottom Elevation with Steam Air Content and 16 lbm/sec-ft^2 Steam Mass Flux - Single Vent Tests at Three Scales

Figure 5-44 Variation of Mean PUP at Pool Bottom Elevation with Steam Air Content and 16 lbm/sec-ft^2 Steam Mass Flux - Single Vent Tests at Three Scales

Figure 5-45 Variation of Mean Chug Frequency with Steam Air Content and 16 lbm/sec-ft^2 Steam Mass Flux - Single Vent Tests at Three Scales

Figure 5-46 Data Traces at 0% Steam Air Content and 4 lbm/sec-ft^2 Steam Mass Flux - 1/4 Scale Single Vent Tests at Three Scales

Figure 5-47 Data Traces at 0.1% Tesam Air Content and 4 lbm/sec-ft^2 Steam Mass Flux - 1/4 Scale Single Vent Tests

Figure 5-48 Data Traces at 0.2% Steam Air Content and 4 lbm/sec-ft^2 Steam Mass Flux - 1/4 Scale Single Vent Test

Figure 5-49 Data Traces at 0.5% Steam Air Content and 4 lbm/sec-ft^2 Steam Mass Flux - 1/4 Scale Single Vent Test

Figure 5-50 Variation of Mean POP at Pool Bottom Elevation with Steam Flux and 130°F Pool Temperature - 5/12 Scale Vents at Two Lengths

Figure 5-51 Variation of Mean PUP at Pool Bottom Elevation with Steam Flux and 130°F Pool Tempertature - 5/12 Scale Vents at Two Lengths

Figure 5-52 Variation of Mean Chug Frequency with Steam Flux and 130°F Pool Temperature - 5/12 Scale Vents at Two Lengths

Figure 5-53 Variation of Mean POP at Pool Bottom Elevation with Pool Temperature and 4 lbm/sec-ft^2 Steam Mass Flux - 5/12 Scale Vents at Two Lenghts

The following Figures are GENERAL ELECTRIC COMPANY PROPRIETARY and have been removed from this document in their entirety.

Figure 5-54 Variation of Mean PUP at Pool Bottom Elevation with Pool Temperature and 4 lbm/sec-ft^2 Steam Mass Flux - 5/12 Scale Vents at Two Lenghts

Figure 5-55 Variation of Mean Chug Frequency with Pool Temperature and 4 lbm/sec-ft^2 Steam Mass Flux - 5/12 Scale Vents at Two Lengths

Figure 5-56 Variation of Mean POP at Pool Bottom Elevation with Pool Temperature and 10 lbm/sec-ft^2 Steam Mass Flux - 5/12 Scale at Two Lenghts

Figure 5-57 Variation of Mean PUP at Pool Bottom Elevation with Pool Temperature and 10 lbm/sec-ft^2 Steam Mass Flux - 5/12 Scale Vents at Two Lenghts

Figure 5-58 Varaition of Mean Chug Frequency with Pool Temperature and 10 lbm/sec-ft^2 Steam Mass Flux - 5/12 Scale Vents at Two Lengths

Figure 5-59 Variation of Mean POP at Pool Bottom Elevation with Steam Air Content and 10 lbm/sec-ft^2 Steam Mass Flux- 5/12 Scale Vents at Two Lengths

Figure 5-60 Variation of Mean PUP at Pool Bottom Elevation with Steam Air Content and 10 lbm/sec-ft^2 Steam Mass Flux - 5/12 Scale Vents at Two Lenghts

Figure 5-61 Variation of Mean Chug Frequency with Steam Air Content and 10 blm/sec-ft^2 Steam Mass Flux - 5/12 Scale Vents at Two Lengths

Figure 5-62 Data Traces at 160°F Pool Temperature and 2 lbm/sec-ft^2 Steam Mass Flux - 5/12 Scale Long Vent

Figure 5-63 Data Traces at 160°F Pool Temperature and 2 lbm/sec-ft^2 Steam Mass FLux - 5/12 Scale Short Vent

Figure 5-64 Data Traces at 10 lbm/sec-ft^2 Steam Mass Flux and 160°F Pool Temperature - 5/12 Scale Long Vent

Figure 5-65 Data Treces at 10 lbm/sec-t^2 Steam Mass Flux and 160°F Pool Temperature - 5/12 Scale Long Vent

Figure 5-66 Pool Temperature Dsitributions at Several Steam Mass Fluxes and 160°F Pool Temperature - 5/12 Scale Long Vent

The following Figures are GENERAL ELECTEIC COMPANY PROPRIETARY and have been removed from this document in their entirety.

Figure 5-67 Pool Temperature Distribution at Several Steam Mass Fluxes and 160°F Pool Temperature - 5/12 Scale Short Vent

Figure 5-68 Data Treces at 8 lbm/sec-ft^2 Steam Mass Flux and 130°F Pool Temperature - 5/12 Scale Short Vent

Figure 5-69 Data Traces at 8 lbm/sec-ft^2 Steam Mass Flux and 130°F Pool Temperature - 5/12 Scale Short Vent

Figure 5-70 Pool Temperature Distribution at 8 lbm/sec-ft^2 Steam Mass Flux and 130°F Pool Temperature - 5/12 Scale Long Vent

Figure 5-71 Pool Temperature Distribution at 8 lbm/sec-ft^2 Steam Mass Flux and 130°F Pool Temperature - 5/12 Scale Short Vent

6. TESTS RESULTS AND DISCUSSION OF MULTIVENT DATA AT 1/10 AND 1/6 SCALE

As an extension to the data base generated in Phase 1, two additional multivent geometries were tested in Phase 2 (19 vents at 1/10 scale and 7 vents at 1/6 scale). Phase 2 multivent data are presented in this section and compared with the single and multiple vent geometry data at the same scales obtained in Phase 1.

The effects of steam mass flux, temperature, and steam air content on multivent chugging are presented in Subsection 6.1. These effects are displayed through the use of data traces of the pool wall bottom elevation pressure, vent static pressure, drywell pressure and vent water level for the single and multivent geometries. Also, quantitative effects are shown through crossplots of mean POP, PUP, chug frequency and the multivent multiplier. The multivent multiplier is defined as the ratio of the mean POP for a multivent geometry to the mean POP for the corresponding single vent geometry at the same scale and for the same test conditions and transducer location. The vent phasing in the multivent geometry is examined in Subsection 6.2.

6.1 MULTIVENT POOL WALL PRESSURES

6.1.1 General Characteristics

Data traces for the 1/10 scale geometries are shown in Figure 6-1 through 6-4 for 1, 3, 7 and 19 vents, respectively, at a steam mass flux of 4 $lbm/sec\text{-}ft^2$, 130°F pool temperature and zero air-content. The amplitude of the pool wall bottom elevation pressure is seen to decrease in the multivent geometries, while the number of chugs in these three second segments of data is slightly greater for the multivent geometries than for the single vent geometry.

The vent static pressure trace in each of the figures was taken from the vent circumferentially adjacent to the pool wall bottom elevation pressure transducer location. The magnitude of the vent pressure fluctuations is approximately the same for the single and multiple vent geometries, indicating that the transient flow induced in each vent during chugging remained constant.

The amplitude of the drywell pressure fluctuations and the height of water reentry in the vent following the chugs decrease from the single vent to the multiple vent geometries.

Sample data traces for the 1/6 scale, 1, 3, and 7 vent geometries are shown in Figure 6-5, 6-6, and 6-7 for the same test conditions as for the 1/10 scale data traces discussed above, i.e., vent steam flux 4 lbm/sec-ft^2, 130°F pool temperature and zero steam air content. The behavior of the 1/6-scale geometries displayed in these data traces is similar to that for the 1/10 scale multivent geometries.

6.1.2 Effect of Steam Mass Flux

The mean POP, PUP and chug frequency data for the 1/10 scale single and multivent geometries as a function of steam mass flux at a pool temperature of 130°F are shown in Figures 6-8, 6-9 and 6-10. The variations of mean POP and PUP with steam mass flux are similar for the single and multiple vent geometries. The highest wall pressures were obtained with the single vent geometry at all steam mass fluxes tested. The mean POP and PUP for the 19 vent geometry lie between the values for the 3 and 7 vent data. In each of the 1/10 scale geometries, chug frequency increases with steam mass flux, with the mean chug frequency for the multivent geometries being slightly higher than that for the single vent geometry.

Figure 6-11 shows the multivent-multiplier for the 3, 7, and 19 vent geometries at 1/10 scale, at several mass flux values and a pool temperature of 130°F. The uncertainty bands for the multivent multiplier are shown on the plot. These bands are indicative of the magnitude of uncertainty in the pressure measurements and do not represent the random nature of the chugging process. Figure 6-11 shows that the multivent multiplier is less than unity for all the multivent geometries over the range of steam mass fluxes shown. In tests with steam mass flux less than 1 lbm/s-ft^2 the multivent multiplier is sometimes greater than unity. However, in all such cases the magnitude of the mean POP for the multivent geometry is less than the uncertainty in the pressure measuring system (approximately ±1 psi) and therefore, the magnitude of the multivent multiplier for those geometries and test conditions is highly uncertain.

It was shown from the Phase 1 data that multiple vents do not chug in phase, and it was concluded that this phase difference accounts for the reduced pressure amplitude at the pool wall for the multiple vent geometries. The reasons for the slight increase in multivent multiplier at 19 vents will be addressed in the final report.

The comparisons between the single and multiple vent geometries at 1/6 scale as a function of steam mass flux are shown in Figures 6-12 through 6-14. The trends in POP, PUP and chug frequency are the same at this scale as those for the 1/10 scale geometries. The effect of number of vents on chug frequency is less pronounced at 1/6 scale than at 1/10 scale. The multivent multiplier for the 1/6 scale, 3 and 7 vent geometries at several steam mass flux values and a pool temperature of 130°F is shown in Figure 6-15. Again, the multivent multiplier is less than unity, although the multivent multiplier for the 7 vent geometry is slightly higher than that for the 3 vent geometry at the 8 lbm/sec-ft^2 steam mass flux, for reasons to be discussed in the final report.

6.1.3 Effect of Pool Temperature

The effect of pool temperature on multivent chugging is shown in Figures 6-16 through 6-18 for the 1/10-scale geometries and Figure 6-19 through 6-21 for the 1/6 scale geometries. Both sets of data are for a steam mass flux of 4 lbm/sec-ft^2 and zero steam air-content. The trends of the mean POP, PUP and chug frequency with pool temperature for the multivent geometries are the same as those for the single vent geometry at both scales. Mean POP and PUP are smaller for the multivent geometries than for the corresponding single vent geometry, and the chug frequencies are higher.

Multivent multipliers for the 1/10 and 1/6 scale geometries are shown in Figure 6-22 and 6-23 at a steam mass flux of 4 lbm/sec-ft^2. The multivent multiplier is less than unity for all cases, and again, the 19 vent geometry shows a slightly higher multivent multiplier than the 7 vent 1/10 scale data at each pool temperature. In this steam mass flux, the multivent multiplier decreases with increasing number of vents at 1/6 scale.

6.1.4 Effect of Steam Air-Content

Trends in the mean POP, PUP and chug frequency with steam air-content are shown in Figures 6-24 through 6-26 for the 1/10 scale geometries and in Figures 6-27 through 6-29 for the 1/6-scale geometries for a steam mass flux of 4 lbm/sec-ft^2. The mean POP and PUP decrease with increasing steam air content for the multivent geometries just as for the single vent geometry. Chug frequency is not significantly affected by steam air-content. The multivent multipliers for the 1/10 and 1/6 scale data are shown in Figures 6-30 and 6-31. Again, the multivent multiplier is less than unity over the range of steam air-content tested.

6.1.5 Summary

In general, the character of the wall pressure signal for the multiple vent geometries is the same as that for the single vents at 1/10 and 1/6 scale. Trends in mean POP, PUP, and chug frequency as a function of the main thermodynamic parameters (steam mass flux, pool temperature, and steam air content) are similar for the single and multivent geometries. The magnitudes of the POP and PUP for multiple vent geometries are smaller than the POP and PUP for the corresponding single vent geometry under the same test conditions.

6.2 VENT PHASING

The three vent geometries tested in Phase 1 showed that not all vents chugged in a given pool chug. Further, the bubble collapses at the individual vents did not occur precisely at the same time - the average time delay between the bubble collapse at the first and last vent in a given pool chug was found to be around 20 msec. Only three vents in the Phase 2 multivent geometries were instrumented with vent static pressure and vent water level transducers necessary for determination of vent phasing. Therefore, it was not possible to obtain quantitative phasing data such as those obtained in Phase 1. However, some qualitative phasing information can be obtained by examining the vent pressure and water level data.

Figure 6-32 shows the pool bottom pressure trace and the static pressure traces for the three instrumented vents in the 1/10 scale 19 vent geometry 1 lbm/sec-ft^2 steam mass flux and 130°F pool temperature. It is seen that for a given pool chug indicated by the pool bottom pressure, vent pressure oscillations do not occur in all three vents. Since vent pressure oscillations are produced by the bubble collapse at the vent exit, the lack of vent pressure oscillations in a vent during a pool chug indicates that bubble collapses do not occur at all vents in a given pool chug. For example, in Figure 6-32, the pool bottom pressure shows that a pool chug occurred at around 42.3 seconds. However, none of the three vent static pressures show any oscillations. Therefore, it can be concluded that at least these three vents did not have bubble collapses in this pool chug.

Further, for pool chugs where all three instrumented vents show vent pressure oscillations, the vent pressure oscillations are not in phase. This indicates that the bubble collapses at the individual vents do not occur at precisely the same time.

The pool bottom pressure and the static pressures in the three instrumented vents at a steam mass flux of 4 lbm/sec-ft^2 are shown in Figure 6-33. At this higher steam mass flux it is seen from these traces that all three vents participate in a greater number of pool chugs compared with the 1 lbm/sec-ft^2 steam mass flux condition (Figure 6-32). This is again consistent with the observations made from the Phase 1 data where it was observed that the percentage of pool chugs in which all vents participate increases with increasing steam mass flux. In Figure 6-33 that the vent static pressure oscillations in the three vents are observed out of phase indicating non-simultaneous bubble collapses.

The occurrence of non-simultaneous bubble collapses at individual vents, however, does not preclude the synchronization of the gross chug. This is because the time window within which the bubble collapse occurs at individual vents in a given pool chug is much smaller than the period between pool chugs. Figure 6-34 shows the data traces for the 1/6 scale 7 vent geometry at

8 lbm/sec-ft^2 steam mass flux and 130°F pool temperature. Distinct pool chugs are observed in the pool bottom pressure trace at nearly regular periods. Further, the drywell pressure shows regular depressurizations corresponding to each pool chug, followed by repressurizations. These regular pressure fluctuations in the drywell pressure indicate that the condensation events at the various vents are synchronized in a gross sense (if the condensation events at the various vents were totally random in time, the drywell depressurizations would be irregular and small in magnitude).

Hence, in closing, qualitative examination of the static pressures in the three instrumented vents indicate that not all vents participate in a given pool chug, although the percentage of pool chugs where all the vents participate increases with steam mass flux. Further, the vent static pressure oscillations are not in phase indicating that bubble collapses at individual vents are not simultaneous. Finally, it appears that the gross chug is synchronized.

The following Figures are GENERAL ELECTRIC COMPANY PROPRIETARY and have been removed from this document in their entirety.

Figure 6-1 Data Traces - 1/10 Scale Single vent test

Figure 6-2 Data Traces - 1/10 Scale 3 Vent Test

Figure 6-3 Data Traces - 1/10 Scale 7 Vent Test

Figure 6-4 Data Traces - 1/10 Scale 7 Vent Test

Figure 6-5 Data Traces - 1/6 Scale Single Vent Test

Figure 6-6 Data Traces - 1/6 Scale 3 Vent Test

Figure 6-7 Data Traces - 1/6 Scale 7 Vent Test

Figure 6-8 Variation of Mean POP at Pool Bottom Elevation with

Figure 6-9 Variation of Mean PUP at Pool Bottom Elevation with Number of Vents - 1/10 Scale Single and Multivent Tests

Figure 6-10 Variation of Mean Chug Frequency with Number of Vents - 1/10 Scale Single and Multivent Tests

Figure 6-11 Multivent Multiplier (Mean POP) at Pool Bottom Elevation - 1/10 Scale Single and Multivent Tests

Figure 6-12 Varaiation of Mean POP at Pool Bottom Elevation with Number of Vents - 1/6 Scale Single and Multivent Tests

Figure 6-13 Variation of Mean POP at Pool Bottom Elevation with Number of Vents - 1/6 Scale Single and Multivent Tests

Figure 6-14 Variation of Mean Chug Frequency with Nubmer of Vents - 1/6 Scale Single and Multivent Tests

Figure 6-15 Multivent Multiplier (Mean POP) at Pool Bottom Elevation - 1/6 Scale Single and Multivent Tests

Figure 6-16 Variation of Mean POP at Pool Bottom Elevation with Number of Vents - 1/6 Scale Single and Multivent Tests

Figure 6-17 Variation of Mean PUP at Pool Bottom Elevation with Number of Vents - 1/10 Scale Single and Multivent Tests

Figure 6-18 Variation of Mean Chug Frequency with Number of Vents - 1/10 Scale Single and Multivent Tests

The following Figures are GENERAL ELECTRIC COMPANY PROPRIETARY and have been removed from this document in th ir entirety.

Figure 6-19 Variation of Mean POP at Pool Bottom Elevation with Number of Vents - 1/6 Scale Single and Multivent Tests

Figure 6-20 Variation of Mean PUP at Pool Bottom Elevation with Number of Vents - 1/6 Scale Single and Multivent Tests

Figure 6-21 Variation of Mean Chug Frequency with Number of Vents - 1/6 Scale Single and Multivent Tests

Figure 6-22 Multivent Multiplier (Mean POP) at Pool Bottom Elevation - 1/6 Scale Single and Multivent Tests

Figure 6-23 Multivent Multiplier (Mean PCP) at Pool Bottom Elevation - 1/6 Scale Single and Multivent Tests

Figure 6-24 Variation of Mean POP at Pool Bottom Elevation with Number of Vents - 1/10 Scale Single and Multivent Tests

Figure 6-25 Variation of Mean PUP at Pool Bottom Elevation with Number of Vents - 1/10 Scale Single and Multivent Tests

Figure 6-26 Variation of Mean Chug Frequency with Number of Vents - 1/10 Scale Single and Multivent Tests

Figure 6-27 Variationof Mean POP at Pool Bottom Elevation with Number of Vents - 1/6 Scale Single and Multivent Tests

Figure 6-28 Variationof Mean PUP at Pool Bottom Elevation with Number of Vents - 1/6 Scale Single and Multivent Tests

Figure 6-29 Variation of Mean Chug Frequency with Number of Vents - 1/6 Scale Single and Multivent Tests

Figure 6-30 Multivent Multiplier (Mean POP) at Pool Bottom Elevation - 1/10 Scale Single and Multivent Tests

Figure 6-31 Multivent Multiplier (Mean PCP) at Pool Bottom Elevation - 1/6 Scale Single and Multivent Tests

Figure 6-32 Data Traces at 130°F Pool Temperature and 1 lbm/sec-ft^2 Steam Mass Flux - 1/10 Scale Vent Test

Figure 6-33 Data Treces at 160°F Pool Temperature and 4 lbm/sec-ft^2 Steam Mass Flux - 1/10 Scale 19 Vents Test

Figure 6-34 Data Treces at 130°F Pool Temperature and 8 lbm/sec-ft^2 Steam Mass Flux - 1/6 Scale 7 Vent Test

7. CONCLUSIONS

Phase 2 of the Scaled Multivent Test Program has extended the data base for single and multivent chugging obtained in Phase 1 and provided the additional data necessary for meeting the program objectives.

In Phase 2, data were obtained on single vent chugging at 1/4 and 5/12 scales. These data were compared with the 1/6 and 1/10 scale single vent chugging data obtained in Phase 1. The major conclusion drawn from this comparison is that the trends in mean POP, PUP and chug frequency with the important thermodynamic parameters - steam mass flux, pool temperature and steam air-content, are similar at all four scales. The magnitude of mean POP decreases with increasing scale, whereas the magnitude of the mean PUP is about the same at all four scales. The mean chug frequency is not affected by scale at lower steam fluxes. At higher steam mass fluxes ($\geq$ 8 lbm/sec-ft^2) there appears to be a trend with scale where the mean chug frequency decreases with scale.

From the data at 5/12 scale for two different vent lengths, it was found that the longer vent geometry had a greater tendency to produce oscillatory-type chugging. Although this tendency towards more oscillatory chugging in the longer vent geometry produces some differences, the overall trends of the mean POP, PUP and chug frequency with the important thermodynamic parameters were similar for the long and short vent geometries.

The two multivent geometries tested in Phase 2 were the 1/10 scale 19 vent and the 1/6 scale 7 vent. It was found that the magnitude of the wall pressures produced by chugging in these multivent geometries was lower than that in the corresponding single vent geometries. That is, the multivent multiplier was less than unity. The variation of the mean POP, PUP and chug frequency with the important thermodynamic parameters for the multivent geometries were similar to those for the corresponding single vent geometries. These findings are consistent with the Phase 1 multivent data.

In closing, the Phase 1 and Phase 2 tests have resulted in the generation of a broad and comprehensive data base on single and multivent chugging. This data base, along with the analyses in progress will provide the necessary justifications for the bounding nature of single cell chugging wall pressures.

8. REFERENCES

1. B. R. Patel, F. X. Dolan, and J. A. Block, "Comparison of Single and Multivent Chugging at Two Scales," NEDE-24781-1-P, January 1980.

2. W. A. Grafton, T. R. McIntyre, and M. A. Ross, "Mark II Pressure Suppression Test Program, Phase II and III Tests," NEDE-13468-P, October 1976.

3. W. J. Bilanin, et al., "Mark II Lead Plant Topical Report - Pool Boundary and Main Vent Chugging Loads Justification," NEDO-23617, July 1977.

4. W. J. Clabaugh, "Sealed Multivent Test Program Plan - Phase 1 Tests," NEDO-23697A, Rev. 1, January 1979.

5. W. J. Clabaugh, "Sealed Multivent Test Program Plan - Phase 2 Tests," NEDO-23697A, Rev. 1, Supplement 1, September 1979.

6. "Fluid Meters - Their Theory and Application," ASME 1971, 6th Edition.

7. B. R. Patel, F. X. Dolan, and J. A. Block, "Conmap Tests Experimental Data Report," TN-297, Creare Report, June 1979.